THE JOURNAL OF THE
ASTRONAUTICAL SCIENCES

VOLUME VIII, NO. 3 FALL 1961

CONTENTS

PUBLISHED BY THE AMERICAN ASTRONAUTICAL SOCIETY, INC.

THE AMERICAN ASTRONAUTICAL SOCIETY, INC.

516 Fifth Avenue, New York 36, New York, U.S.A.

THE AMERICAN ASTRONAUTICAL SOCIETY

The American Astronautical Society, founded in 1953 and incorporated in New York State in 1954, is a national scientific organization dedicated to advancement of the astronautical sciences. The society considers manned interplanetary space flight a logical progression from today's high-performance research aircraft, guided missile, and earth satellite operations. The scope of the society is illustrated by a partial list of the astronautical fields of interest: astronavigation, biochemistry, celestial mechanics, cosmology, geophysics, space medicine, and upper atmosphere physics, as well as the disciplines of astronautical engineering including space vehicle design, communications, control, instrumentation, guidance, and propulsion. The aims of the society are to encourage scientific research in all fields related to astronautics and to propagate knowledge of current advances. Promotion of astronautics in this way is accomplished by the society largely through its program of technical meetings and publications.

AFFILIATIONS

AAS cooperates with other national and international scientific and engineering organizations. AAS is an affiliate of the American Association for the Advancement of Science and a member organization of the International Astronautical Federation.

MEMBERSHIP REQUIREMENTS

All persons having a sincere interest in astronautics or engaged in the practice of any branch of science, which contributes to or advances the astronautical sciences, are eligible for one of the various grades of membership in the Society. Requirements are tabulated below. A special category of Student Membership has been authorized for full time students or those under 18 years of age. A nominal membership fee of $5.00 is made in such cases to cover publications. The Directors of the Society may elect as Fellows of the Society those who have made direct and significant contributions to the astronautical sciences. Information regarding individual membership as well as Corporate and Benefactor Membership may be obtained by writing the Corresponding Secretary at the Society address.

Grade	Contribution To Astronautics	Experience or Scientific Training*	Annual Dues
Affiliate Member	Interest	none required	$8
Member	Active Interest	8 years	$10
Senior Member	Recognized Standing and Direct Contribution	10 years	$15

* A Bachelor's, Master's or Doctor's degree in any branch of science or engineering is equivalent to four, six or eight years of experience, respectively.

The *Journal of the Astronautical Sciences*

Director of Publications, George R. Arthur
Editor, Robert M. L. Baker, Jr.
Managing Editor, George J. Clark

Published quarterly by the AMERICAN ASTRONAUTICAL SOCIETY, INC. at 428 E. Preston Street, Baltimore 2, Maryland

Address all Journal correspondence to Box 24721, Los Angeles 24, Calif.

Subscription Rates: One year $5.00; foreign $6.00; single copy $1.25. The Journal is published quarterly.

Second-class postage paid at Baltimore, Maryland.

Measurements of Sheath Currents and Equilibrium Potential on the Explorer VIII Satellite[1]

R. E. Bourdeau, J. L. Donley, G. P. Serbu, and E. C. Whipple, Jr.[2]

Abstract

Presented are experimental data obtained from the Explorer VIII satellite of five parameters pertinent to the problem of the interaction of space vehicles with an ionized atmosphere. The five parameters are: photoemission current due to electrons emitted from the satellite surfaces as a result of solar radiation, electron) and positive ion currents due to the diffusion of charged particles from the medium to the spacecraft, the potential of the vehicle relative to the medium, and the ambient electron temperature. Included in the experimental data is the aspect dependence of the photoemission and diffusion currents. The observations then are used to postulate certain characteristics of the satellite's plasma sheath.

Introduction

This report is concerned with one type of interaction between a space vehicle and an ionized atmosphere. Specifically, it deals with the equilibrium potential of the Explorer VIII satellite and the current exchange between this spacecraft and the ionosphere. The experimental data herein presented are fundamental to the characteristics of the plasma sheath surrounding a space vehicle. The report deals, then, with an interaction localized to the proximity of the body. The data should be important to the evaluation of other types of interactions that have been postulated since all disturbances must begin right at the body itself.

Both the characteristics of the ionosphere and of the space vehicle contribute to their mutual interaction. For an orbiting satellite, the sheath properties are determined by the following factors:

A. Parameters of the undisturbed ionosphere
   (1) The ambient electron temperature (T_e);
   (2) the random electron current density (J_e);
   (3) the random ion current density (J_+); and
   (4) the magnetic field (B).

B. Factors due to presence of the satellite
   (1) Radio-frequency fields used for telemetry transmissions;
   (2) conductivity of the surface;
   (3) photoemission current density (J_p) due to solar radiation; and
   (4) the satellite motion.

For a conducting body at rest where rf and magnetic fields and solar radiation may be neglected, the equilibrium potential is given by:

$$\phi_0 = \frac{-kT_e}{e} \ln \frac{J_e}{J_+}, \tag{1}$$

where k is Boltzmann's constant and e the electronic charge. Since $J_e \gg J_+$, ϕ will be negative resulting in a positive ion sheath with a thickness related to T_e and the electron concentration, N_e.

Consider now the factors introduced by the presence of the satellite. It is known that antennas radiating rf fields can, by rectifying process, cause a larger negative potential than would be expected from Eq. (1). However, experimental observations made from rockets (Ref. 1) during rf silence have been compared with data taken in the same flight during rf transmissions. These data show that for the amount of power (100 mw) and the frequency (108 mc) used by the Explorer VIII telemetry system the rf field effect due to telemetry transmissions can be neglected.

The satellite motion affects the sheath in the following manner. The velocity is much greater than that of the positive ions. Consequently, the random ion current is essentially incident over that portion of the satellite surface projected in the direction of motion. The electron current should also be a maximum at the forward surface although the effect will be smaller because of the higher thermal velocities of the electrons.

The electron current is also affected by the magnetic field, as Beard and Johnson (Ref. 2) have described. The motion of the satellite with velocity $\mathbf{V}$ through the magnetic field produces an induced potential that is a function of position on the satellite surface,

$$\phi = \phi_0 + (\mathbf{V} \times \mathbf{B}) \cdot \mathbf{d}, \tag{2}$$

where ϕ_0 would be the satellite potential with no mag-

[1] Presented at the American Astronautical Society Meeting 7 March, 1961.

[2] Goddard Space Flight Center, NASA, Greenbelt, Md.

netic field, and $\mathbf{d}$ is the vector distance of any point on the surface from the satellite center. A satellite potential of ϕ_0 will be measured at all points which lie on a plane passing through the satellite center perpendicular to $\mathbf{V} \times \mathbf{B}$. All other points will either be more positive or more negative than ϕ_0 depending on which side of this plane they are situated. The electron current would be expected to be a maximum where ϕ is most positive which would be near the point corresponding to the direction $\mathbf{V} \times \mathbf{B}$.

The photoemission current density, J_p, tends to make ϕ_0 more positive. At low electron concentrations, it is possible that photoemission can predominate resulting in a positive ϕ_0 and a sheath containing electrons.

If the effects of the magnetic field and satellite velocity on the electron current can be neglected, then the following expression for the satellite potential is valid:

$$\phi_0 = -\frac{kT_e}{e}\ln\frac{J_e S}{\int J_+ \, dS + \int J_p \, dS}, \qquad (3)$$

where the integration is over the satellite surface S. To take into account the variations in electron current, it is necessary to go back to the fundamental equation for current balance:

$$\int J_e \, dS = \int J_+ \, dS + \int J_p \, dS. \qquad (4)$$

This report will present experimental values obtained from the Explorer VIII satellite of the electron diffusion current, i_e, the ion diffusion current i_+, and the photoemission current, i_p, as a function of the orientation of those points relative to the velocity, solar and magnetic field vectors. Also presented are measured values of ϕ and T_e. These experimental observations then are used to postulate a qualitative model of the plasma sheath and a quantitative model of the current exchange between the satellite and the medium.

The Explorer VIII Satellite

The Explorer VIII Satellite was launched from Cape Canaveral on 3 November 1960, onto an orbit with a 50° inclination, a perigee of 425 kilometers and an apogee of 2300 kilometers. It had a planned active life of two months. The primary mission of this Ionosphere Direct Measurements Satellite, which is only incidental to this report, was the in-situ measurement of electron density and temperature and positive ion concentration and mass.

A photograph of the satellite, highlighting the characteristics pertinent to this discussion is presented in Figure 1. The aluminum shell consists of two truncated cones joined at the equator by a cylinder. It is 30 inches in diameter at the equator and 30 inches high. Non-conductive thermal coatings are located

Fig. 1. Ionosphere direct measurements satellite (Explorer VIII).

on both cones in a pattern conducive to the maintenance of an equipotential surface. Retracted a[re] two ten-foot wires which served as a shortened dipo[le] for an rf impedance experiment designed to measu[re] N_e. A combined solar-horizon seeker provided su[p]porting information on the satellite orientation.

Data from only four of the satellite's many senso[rs] are considered in this presentation. They are:

(1) an ion current monitor, responsive only to th[e] incoming positive ions;

(2) an electron current monitor, responsive to th[e] sum of the incoming electron current an[d] outgoing photoemission current;

(3) a total current monitor, responsive to all thr[ee] types of current;

and

(4) an electron temperature probe, responsive on[ly] to electron current and which measures [N_e] and T_e.

The locations of these four sensors relative to th[e] aspect sensor are shown in Figure 2. All but the electro[n] temperature probe are centered on the equator. Th[e] latter sensor is positioned near the forward end of th[e] spin axis as shown in Figure 1.

In order to evaluate in detail the simultaneou[s] effect of all the sheath-influencing factors listed in th[e] introduction, a single set of conditions was chose[n] where favorable satellite orientation permits clea[r] delineation of the dependency of the ion, electron, an[d]

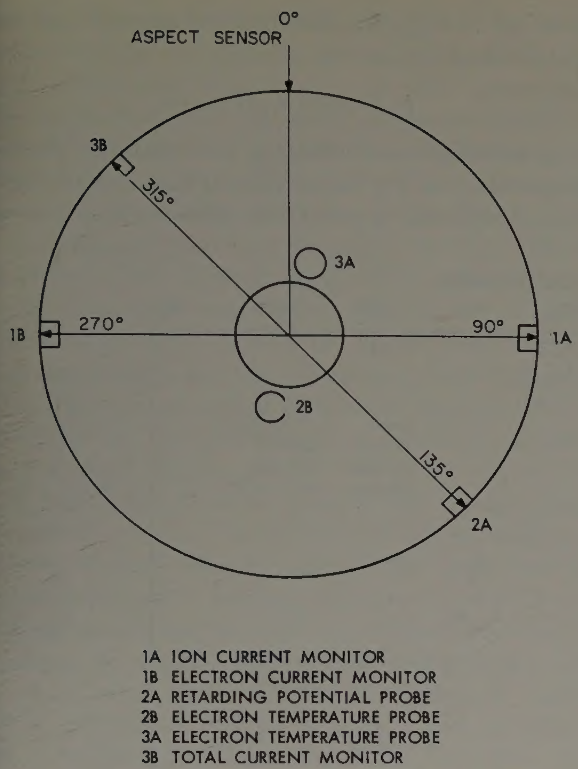

FIG. 2. Sensor locations (Explorer VIII Satellite)

photoemission currents on the location of the velocity, solar and magnetic field vectors. Consequently, all of the reported data will be for the orientation described by Figure 3. Of major importance is that the velocity and solar vectors are separated by 159°. This permits separate scanning of the solar and velocity dependent quantities as the satellite spins. The solar elevation angle was 33° on the upper cone and the velocity vector depression angle was 15° on the lower cone. All the data were acquired within two minutes of 22:57 UT on 27 November 1960, at which time the satellite altitude was 1000 km and its geographic coordinates 33°N and 84°W. The spin rate was 21.4 rpm at this time.

Measured Values of Positive Ion Current

The positive ion current flowing from the ionosphere to the satellite was monitored by a sensor shown schematically in Figure 4. The sensor is constructed in planar geometry and contains three parallel electrodes. The outermost grid is flush with and electrically connected to the satellite skin. The inner grid is biased negatively to suppress photoemission from the collector and to remove incoming electron current from the measured collector current. This collector current i_+ is related to $(i_+)_s$, the current incident at the skin, by

$$i_+ = \alpha_+(i_+)_s\,, \tag{5}$$

where α_+ is the combined electrical transparency of the two grids for positive ions.

Plotted in Figure 5 is the experimental collector

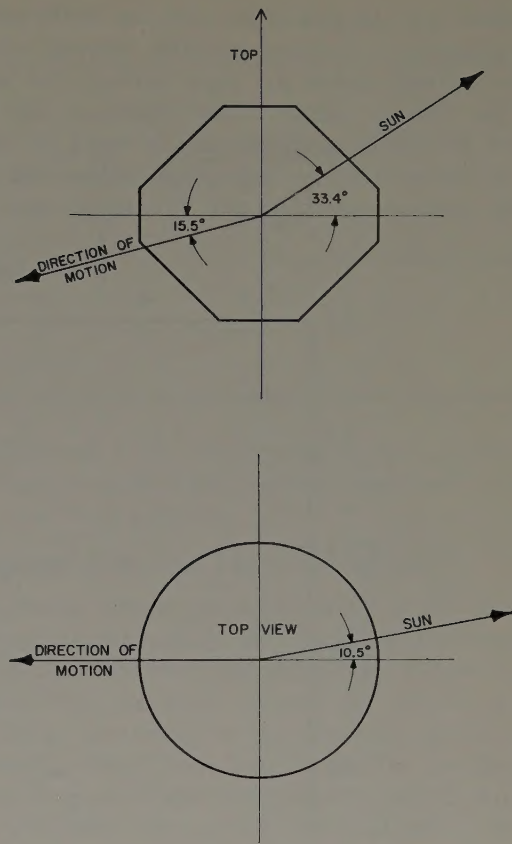

FIG. 3. Satellite orientation (22:57 UT, 27 November 1960)

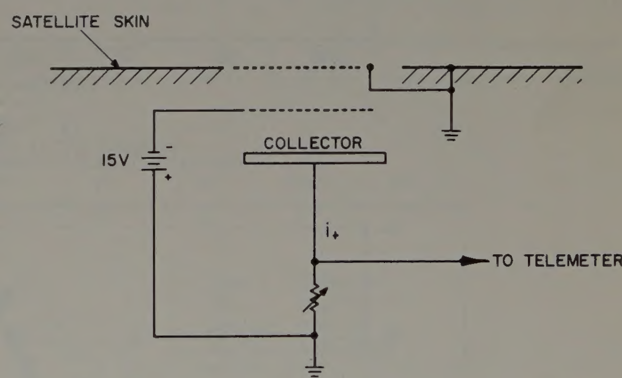

FIG. 4. Ion current monitor (Explorer VIII Satellite)

current as a function of the azimuth angle of the sensor relative to the velocity and solar vectors. The absence of a current when the sensor is pointed at the sun is proof that suppression of photoemission from the collector has been successfully accomplished. The behavior of i_+ relative to the velocity vector is in good agreement with that predicted by Whipple (Ref. 3) in the following general equation which takes into account all values of the satellite-to-ion velocity ratio:

$$i = \alpha NeA\left[V\cos\theta\left(\frac{1}{2} + \frac{1}{2}\operatorname{erf} x\right) + \frac{a\exp^{-x^2}}{2\sqrt{\pi}}\right], \tag{6}$$

where

$$x = \frac{V\cos\theta}{a} - \sqrt{\frac{\phi e}{kT}},$$

and where A is the area of the collector, N the particle concentration, a the most probable thermal velocity of the particle, and θ the angle between the sensor and the velocity vector. This expression has been derived for plane geometry and is valid for either ions or electrons if the appropriate values and signs for the symbols are observed. For angles less than about 45° in Figure 5 the observed currents are fitte[d] by the reduced equation:

$$i_+ = \alpha_+ A N_+ e V \cos\theta. \quad (7$$

Using an inflight calibration of the combined electric[al] transparency of the two grids (92%), a value for N of $1.3 \times 10^4/\text{cm}^3$ is computed. This is consistent wi[th]

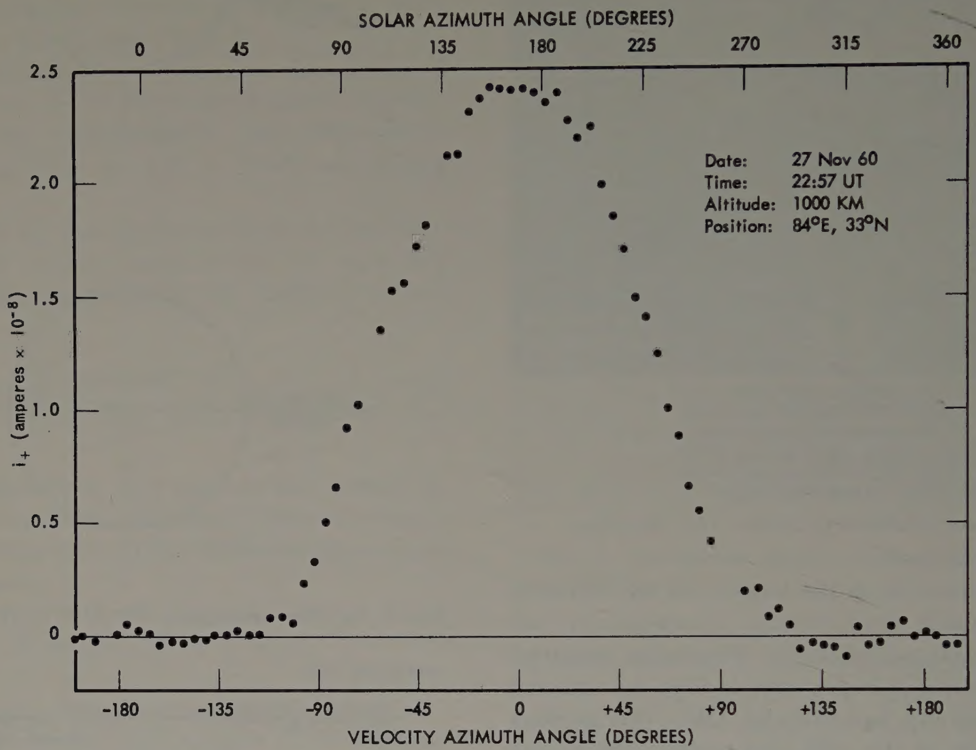

$i_+ = \alpha_+(eAN_+ V \cos\theta),\ |\theta| < 45°$

FIG. 5. Ion current as a function of aspect (Explorer VIII Satellite)

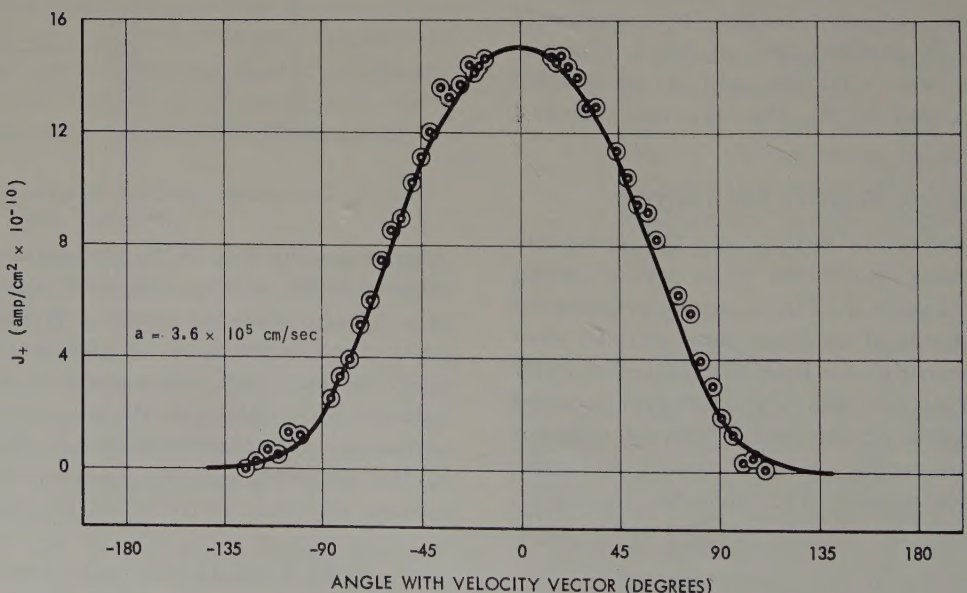

$$J_+ = \alpha_+ e N_+ V \cos\theta \left[1/2 + 1/2 \,\text{erf}\left(\frac{V\cos\theta}{a}\right) + \frac{a\, e^{-\left(\frac{V\cos\theta}{a}\right)^2}}{2\sqrt{\pi}\, V\cos\theta} \right]$$

FIG. 6. Variation of positive ion current density with angle relative to velocity vector of satellite

electron concentrations obtained from the rf impedance probe experiment also carried on Explorer VIII. Ionosonde data taken at this geographical position and at this time yield an electron density of 7×10^5 el/cm^3 at an altitude of about 300 km. The positive ion concentration measured from the satellite agrees with this value, assuming an ionospheric model with a neutral gas scale height of 60 km, diffusive equilibrium, and a predominant 0^+ constituent.

One important qualitative conclusion related to sheath characteristics can be made from Figure 5. The absence of a positive ion current on the side away from the velocity vector is definite experimental evidence for an electron sheath immediately adjoining the vehicle at this location.

In Fig. 6 are plotted values of ion current density computed from i_+/A as a function of the total angle relative to the velocity vector. The solid line is a theoretical curve based on Equation 6, with $\phi = 0$. The agreement between the observed currents and the equation is evident. However, in order to get agreement for angles greater than 45 degrees, a value of 3.6×10^5 cm/sec had to be used in the equation for the most probable ion thermal velocity. This value corresponds to an anomalously high ion temperature if only 0^+ is assumed, but is reasonable if there is a significant amount of H^+, implying that at 1000 km, the satellite is near the transition region between the upper ionosphere and the protonosphere. However, the most probable explanation for the fact that the measured ion current for $\theta 745°$ is higher than that predicted

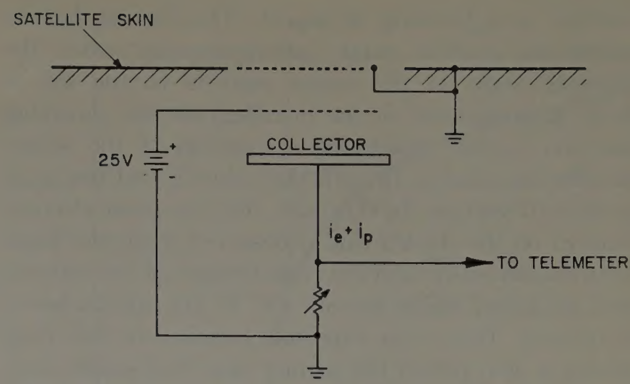

Fig. 7. Electron current monitor (Explorer VIII Satellite)

by Equation 6 for a reasonable temperature is that the negative satellite attracts ions that would otherwise not have been collected.

Measured Values of Electron Current

A sensor responsive to the sum of the incoming electron current and the outgoing photoemission current is illustrated schematically in Figure 7. It is mechanically identical to the ion current monitor but differs electrically in that the inner grid is biased positively rather than negatively. The positive bias serves to remove the incoming ion current from the measured collector current. The collector current is given by:

$$i = i_e + i_p = \alpha_e(i_e)_s + \alpha_p(i_p)_s , \qquad (8)$$

where α_e and α_p are the respective grid transparencies.

Plotted in Figure 8 is the experimental collector

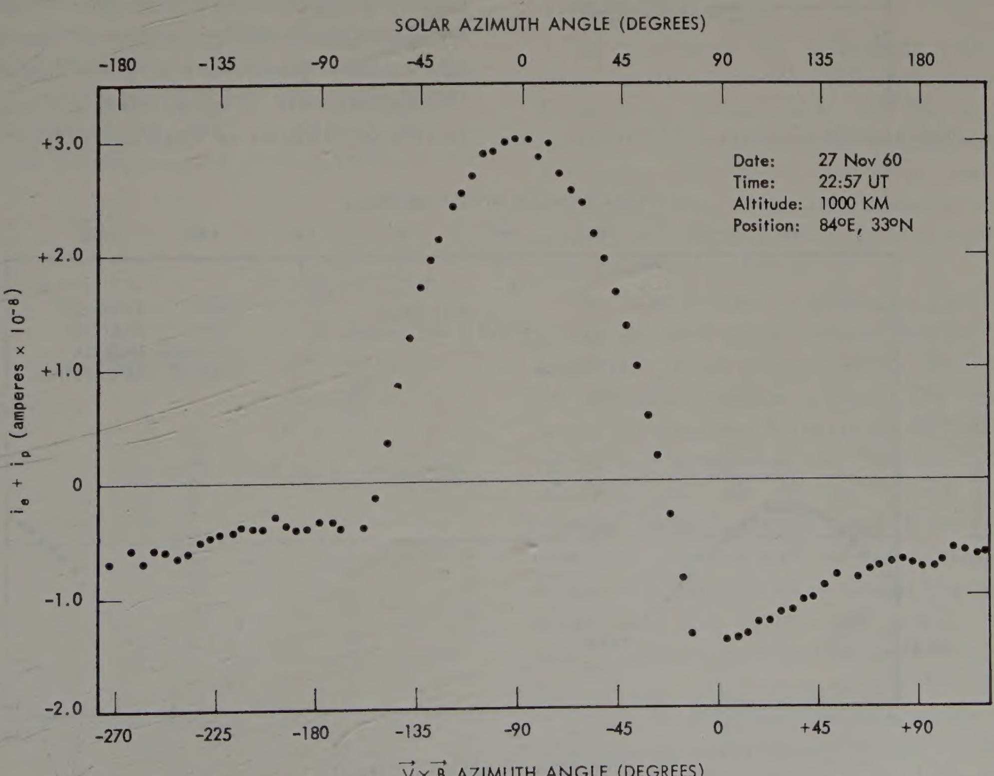

Fig. 8. Electron current as a function of aspect (Explorer VIII Satellite)

current as a function of aspect. The current has its maximum positive value (photoemission) when the azimuth angle of the sensor relative to the sun is zero. As postulated in the introduction, the incoming electron current should be a function of the sensor orientation relative to both the velocity and the magnetic field vectors. In this case, the maximum electron current on the shaded side is observed when the angle between the sensor and the cross-product of the velocity and magnetic fields vectors ($\mathbf{V} \times \mathbf{B}$) approaches a minimum. This is as expected because at this time during a spin period the surface near this sensor location would be at its most positive point.

Measured Values of Total Current

The total current to the satellite was measured at its equator by the sensor illustrated in Figure 9. It consists simply of a collector flush with and insulated from the satellite skin. This collector current is given by

$$i = i_t = (i_e)_s + (i_+)_s + (i_p)_s\,. \tag{9}$$

It represents then, the sum of the effects of Figures 5 and 8, except that the overall amplitude of each component is larger since no grid transparencies are involved.

The total current at the point of measurement is plotted as a function of aspect in Fig. 10. It is in definite agreement with the predominant features of the graphs in Figures 5 and 8. Specifically, the current peaks in the positive direction when the solar angle is zero because of photoemission. The current peaks again in the positive direction for a velocity azimuth angle near zero. The peak here is due to the "ram effect" upon which the positive ion current is largely dependent. The displacement from the zero angle point is due to the influence of the electron current in this region. Finally, a peak current in the direction of an incoming electron current occurs when the angle between the sensor and the cross-product of the velocity and magnetic field vectors ($\mathbf{V} \times \mathbf{B}$) approaches a minimum.

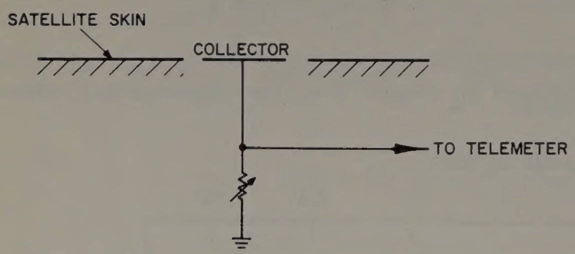

FIG. 9. Total current monitor (Explorer VIII Satellite)

The satellite spin permits examination of the separate behavior of each of the three currents which comprise the total current curve. This in turn makes it possible by comparison of Figure 10 with Figures 5 and 8 to assign an electrical transparency to the grids used in the ion and electron current monitors. This in-flight calibration shows that the combined electrical transparency for positive ions of two parallel grids is approximately that of the optical transparency. On the other hand, the electrical transparency for electrons is only about 30 percent of the optical transparency. This is an important observation in the evaluation of electron temperature data which are discussed in a later section.

A significant quantitative value derived from Fig. 10 is the measured value of the photoemission current density (5×10^{-9} amps/cm^2) taken right at the vehicle surface for a minimum solar angle. This value can be compared with the random electron current density computed from ionospheric models to predict an approximate altitude where the spacecraft potential can become positive. For most ionospheric models, this should occur at about 4000 km, not too far above the apogee altitude of Explorer VIII.

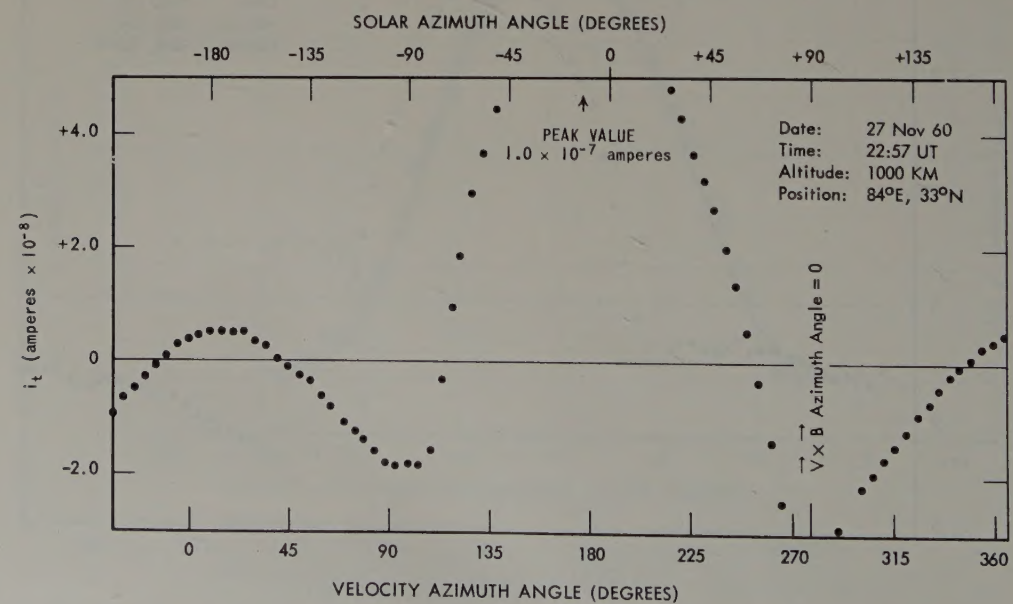

FIG. 10. Total sheath current as a function of aspect (Explorer VIII Satellite)

Measured Values of Electron Temperature and Equilibrium Potential

The sensor illustrated schematically in Figure 11 was used on a time-sharing basis to alternately monitor the incoming electron current at the sensor location and to obtain in the other half of its duty cycle electron temperature and equilibrium potential. It consists of two electrodes, a grid, and a collector. The collector is biased positively to remove photoemission and incoming ion current from the measured collector current. During one phase the grid is kept at the skin potential, thus permitting a measurement of the incoming electron current as a function of aspect. During the other time phase the grid potential relative to the satellite skin is varied from -1.2 to $+8$ volts to obtain ϕ and T_e. The period of the grid voltage sweep (0.2 seconds) is kept small so that the collector current can be studied as a function of the grid voltage for small changes of orientation. At the satellite spin rate, it was possible to obtain a volt-ampere curve for a change in orientation of about 25°.

Presented in Fig. 12 is a typical volt-ampere curve taken during the phase when the potential of the grid relative to the satellite skin was varied in accordance with the waveform illustrated in Figure 11. The electron current is plotted on a logarithmic scale. The shape of the curve is in good agreement with Langmuir probe theory. Two distinct slopes in the regions where the grid is below and above the plasma potential are apparent. The slope of the curve when the grid potential is negative is a measure of the electron temperature. The satellite potential is generally taken as the negative value of either the point where the curve departs from this slope or the point of intersection of the two slopes. For the illustrated curve, an electron temperature of 1800° ± 300° K and a satellite potential between 0 and -0.15 volts is obtained. The error quoted in the temperature is due to the limited resolution.

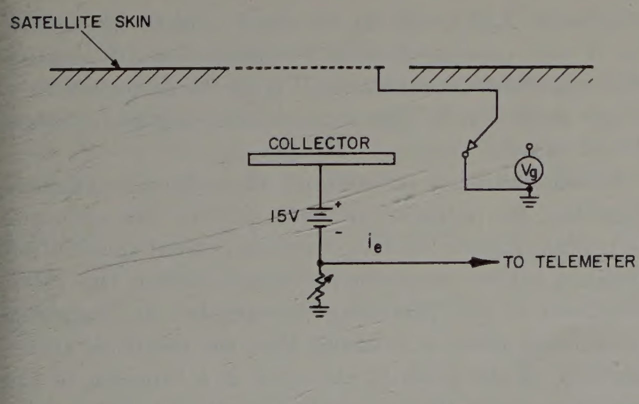

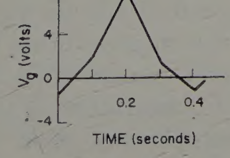

FIG. 11. Electron temperature probe (Explorer VIII Satellite)

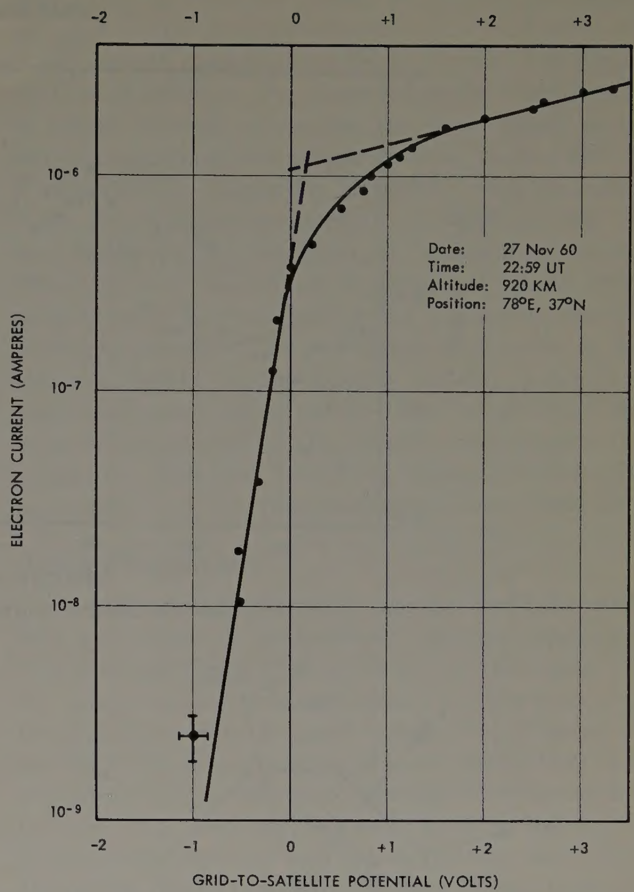

FIG. 12. Typical volt-ampere curve for electron temperature probe (Explorer VIII Satellite).

Not presented are additional volt-ampere curves taken at this time for different sensor orientations. These other curves show that as the satellite spins, the same values of electron temperature are obtained. The major difference is the current read at the plasma potential. These values are consistent with the electron current behavior when the grid is maintained at zero volts as shown in Fig. 13.

The large scatter of points in Fig. 13 compared to all the previous graphs occurs because an electrometer sensitivity range is used where the input voltage to the telemetry system is small. The scatter, therefore, is due to random fluctuations of the telemetry subcarrier at low signal levels. Despite this difficulty, it is apparent that the electron current peaks when the velocity vector azimuth angle is zero. From this observation, together with an examination of the relative values of V and ϕ in Eq. 6, it can be concluded that the potential of the upper cone relative to the medium must be either close to zero as indicated above or can even become positive as the satellite spins.

Figure 14 describes the orientation of the satellite with respect to the magnetic and velocity vectors and demonstrates that this implication is verified. The sensor on the upper cone always remains on the "posi-

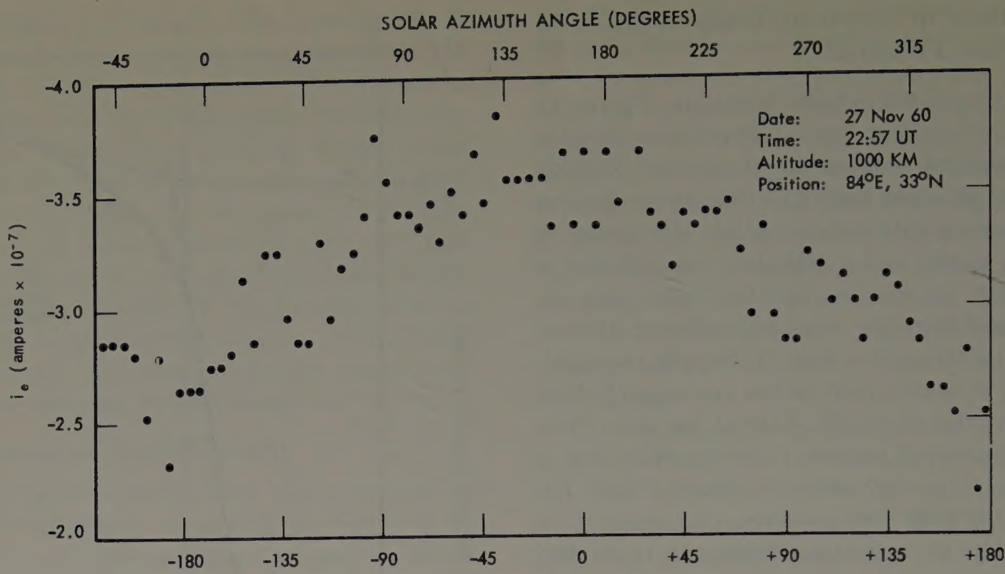

FIG. 13. Electron current as a function of aspect

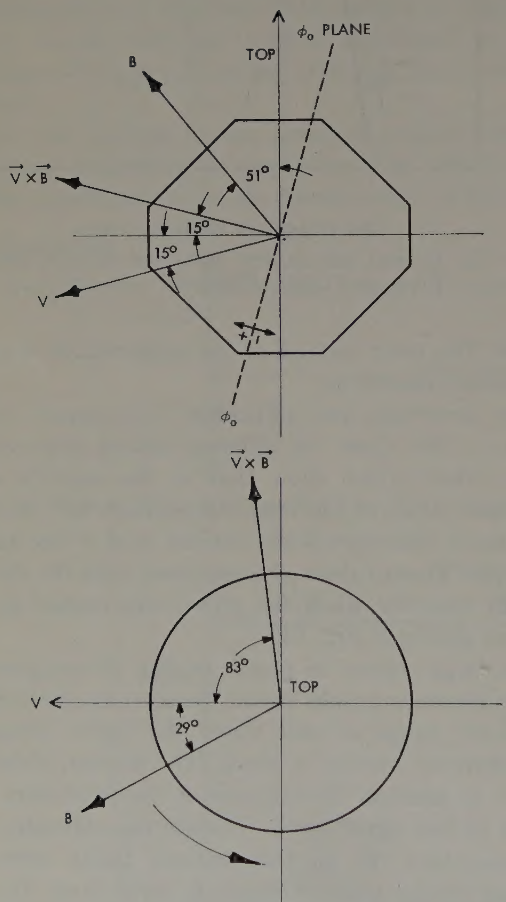

FIG. 14. Orientation of satellite with respect to magnetic and velocity vectors (Explorer VIII Satellite).

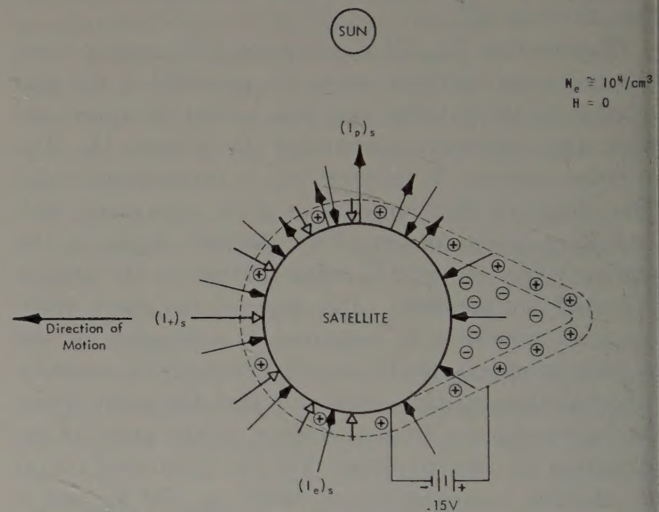

FIG. 15. Qualitative satellite sheath model postulated from experimental data.

tive" half of the satellite, that is, the side that is positive with respect to ϕ_0. Moreover, the change in the distance from the ϕ_0 plane is only 24 cm corresponding to a change in potential of about 0.04 volts. In contrast, the potential on the equator changes by at least 0.14 volts and becomes more negative than ϕ_0. (Values of 7.4×10^5 cm/sec for V and of 0.30 gauss for B were used in the above computation.) Note also that the electron current in Figure 13 is consistently larger than that to the sensor on the equator, as one would expect.

It remains to be pointed out that these conclusions regarding the potential are necessary but not sufficient to explain Figure 13. The observed current modulation requires a lower electron temperature than the 1800° discussed in the preceding paragraphs. As suggested previously, there is evidence that the electrical transparency of the grids to electrons is a function of the electron energy, the fast electrons getting through more readily. This would tend to enhance any current modulation present, and it is suggested that this is occurring here. A changing grid transparency may also affect the determination of temperature. A thorough evaluation of the grid transparency effect on the electron temperature measurement is not yet completed.

Sheath Characteristics Postulated from Experimental Observations

It is concluded that the experimental data from the various sensors are mutually consistent. These data can be used to postulate a qualitative model of the sheath characteristics and a quantitative model of the current exchange between the satellite and the medium.

First, the value of the satellite potential on the upper cone is between 0 and -0.15 volts. The satellite surface is not equi-potential. The motion of the satellite through the magnetic field causes an induced potential so that the potential is very close to zero or positive in the $\mathbf{V} \times \mathbf{B}$ direction and correspondingly more negative at the other end.

The potential distribution on the surface has a marked effect on the observed electron current, with most electrons incident at the more positive end. It should be noted that there was a net electron current to the skin even when the current flow was perpendicular to the magnetic field. A qualitative model of the sheath surrounding the satellite is illustrated in Fig. 15, showing also the effects of solar and velocity vector orientations on the various current exchanges. The electron current shows a ram effect due to the satellite motion if the frontal surface is favorably situated with respect to the more positive end of the satellite.

The positive ion current density is a function only of the angle between the surface normal and the satellite velocity vector. The absence of this current behind the satellite indicates that there is an electron sheath or wake adjoining the rear surface. If it is assumed that the wake is in the form of a cone, its size may be estimated from the ratio of satellite to ion velocities and the satellite diameter. In this case the cone has a half-angle of about 25° and extends back a distance of about one satellite radius. A positive ion sheath surrounds the front of the satellite and should envelope both the satellite and the electron wake. The thickness of the ion sheath would be comparable to one Debye length which is computed to be 2.5 cm.

Finally, there is a photoemission current on the satellite surfaces facing the sun. This current is important in considering the current balance to the satellite and thus the equilibrium potential. However, photoemission does not appear to disturb the sheath adjacent to the emitting surface.

The sheath model illustrated in Figure 15 is for an altitude of 1000 km. The measured positive ion density is $1.3 \times 10^4/\mathrm{cm}^3$. A neutral gas scale height of 60 km corresponding to a temperature of about 1100° K is indicated by comparison of this N^+ with ionosonde data. An electron temperature of 1800° $\pm$ 300° K was measured by the electron temperature probe. However, this value could be influenced by the effect on the probe's grid transparency of a changing electron retarding potential. The percentage modulation of the electron current by the satellite velocity indicates a somewhat lower value for T_e. The behavior of the positive ion current at the satellite sides suggest the possibility that the transition region between the ionosphere and the protonosphere is near 1000 km.

Acknowledgments

It is difficult to list the many agencies and individuals who contribute to a successful satellite operation. The Marshall Space Flight Center was responsible for the launch vehicle and operations. Its Guidance and Control Laboratory designed and fabricated the satellite shell, the despin and separation mechanisms, and the power supply and also supervised environmental testing. The Payload Systems Division of GSFC provided the telemetry and aspect systems. The GSFC Operations Control and Data Systems Design Branches were responsible for data acquisition and data reduction.

Dr. R. C. Waddell and Mr. W. J. Archer of GSFC were responsible for the instrumentation associated with the experiments. Mr. C. R. Hamilton of GSFC acted as project coordinator. Also acknowledged are the helpful discussions with Dr. S. J. Bauer of GSFC, Dr. C. A. Pearse of NRL, and the services of Mrs. Helen Wetklow in the preparation of the text.

References

1. Smith, L. G., private communication.
2. Beard, D. B. and Johnson, F. S., "Charge and Magnetic Field Interaction with Satellites," JGR, January 1960.
3. Whipple, Jr., E. C., "The Ion-Trap Results in Exploration of the Upper Atmosphere with the Help of the Third Soviet Sputnik," IRE Proceedings, November 1959.

Furthering Basic Biological Knowledge Through Space Research[1]

June Lee Biedler[2]

Abstract

The advent of the "space age" has resulted in both the opportunity and the necessity for extended research in various areas of science. That biological science is gathering impetus in certain directions, some of them new, is illustrated by the results of a survey taken for the purpose of this report. There is a manifest need for an interdisciplinary approach to space research whereby those working in the biological sciences will need to further their acquaintance with engineering possibilities and engineers with the requirements of biologists.

Introduction

It seems timely to assess the possible contributions of space exploration to the furtherance of basic biological knowledge—knowledge which is derived from the analytical or observational study of life processes, be they in unicellular organisms such as bacteria or certain of the algae, or in higher plant or animal forms such as tomato plants or mice. While not excluding man as a worthy representative of the biological world, in general the medical or physiological, social or psychological considerations of man-in-space are not pertinent to this discussion. Many of the present studies and projected plans are directly related to that goal—the survival and sustenance of man in the space vehicle or in the extraterrestrial environment. But it is the other side of the coin which concerns us here—the fundamental knowledge which is now increasing and which can be extended by the pursuit of this objective.

Space as a Biological Laboratory

Just what are some of the physical factors unique to the space environment that may make possible an extended understanding of certain biological mechanisms, or may even lead to entirely new concepts? There are kinds and intensities of cosmic and solar radiation, various planetary environments, high vacuum to the order of 10^{-18}, zero-gravity, and so forth. The possibilities of space research have excited those few biologists who have followed the development of space vehicles, not because such research will necessarily bring a simple solution or sudden enlightenment to persistent biological questions, but because there is provided a means of observing terrestrial life mechanisms away from certain constant and inescapable influences in the earth environment, as well as a possibility of discovering mechanisms which have originated entirely outside of these influences.

Implications of Zero-gravity

The physical factors involved are well known to engineers and other physical scientists. Possibly the most important of these, at least at this incipient phase of the "space age," is zero-gravity, the reduction or complete absence of the gravitational force. We are able to reproduce the converse of this state, an increase in gravitational pull, by means of the centrifuge. However, we cannot with validity extrapolate back to the zero-gravity state. Nor can we with complete surety and accuracy simulate this state, although attempts at an approximation to zero-gravity are being made and are worthwhile. Of the greatest importance at present is the effect on man of this entirely strange factor. But how can we begin to understand the possible or even the observed effects upon the highly organized, complex human being before we are able to know if or how certain readily observable biological phenomena are altered.

What effect has zero-gravity on cellular division? For example, it is known that in a given nutritional milieu at a controlled pH, at a constant 37° C temperature, a certain strain of human cancer cells grown in glass culture flasks will divide with an average generation time of 22 hours. Will a change from 1g to 0g alter this division time? Some biologists would say yes, probably; while others would say no, there could not be the slightest effect. The point is, this question cannot be answered on earth. There is a strain of bacteria, *Escherichia coli*, commonly present in our intestinal flora, which will, under optimal conditions, divide approximately every 30 minutes. Would this division time be affected? Certainly a simple question and a relatively simple one to answer from the point of view of experimental design for a space vehicle; but has this question been as yet satisfactorily answered?

What is the effect of zero-G upon embryological de-

[1] Presented to the New York Section of the American Astronautical Society, the New York Academy of Sciences, November 30, 1960.

[2] Research Associate, Sloan-Kettering Institute, Walker Laboratory, Rye, N. Y.

velopment? There are some classical experiments which it would be well to reassess under new conditions. For example, the embryologist may turn the fertilized frog egg upside down to see if the change in polarity of the early embryo influences the development of the tadpole. It turns out that during a certain critical period at least it does—the cleavage of the egg and the tadpole, if formed at all, are abnormal. Exactly why is not known. What would be the effect of the elimination of the constant gravitational pull? It is a fascinating question, and the answer may well illuminate this little understood problem.

Present State of Biological Science

In the foregoing we have discussed the biologists' interest in extending knowledge of biological processes. It might be instructive to mention the state of the art of biological science as compared with that of the physical sciences, since this bears on later remarks concerned not so much with the relationship between the biological and physical sciences as with the communication between biologists and the physical and engineering scientists.

Perhaps it is not widely realized how great is the abundance of uncertainties and unknowns in the understanding of life processes. In biology there are few general laws, whereas physical science has advanced to the state where there is a great body of laws which may be expressed in mathematical terms and by which phenomena may be predicted with complete accuracy. A well-known characteristic of biological phenomena is their variability. Lack of perception of biological unknowns on the part of engineers and those planning space missions may result in insufficient lead time for the gathering of biological data upon which orderly progression of man-in-space missions depends. Credit is given to biologists and medical scientists for possessing information or understanding, credit which unfortunately is as yet so often undeserved. This is the reason why there can be few ready-made answers to problems posed by even our next steps in space flight. Compounding the problem may also be political pressures, which mitigate against the freedom always necessary to the pursuit of basic research.

There needs to be discernment and definition of the objectives of research in space, and perhaps the realization that the accumulation and dissemination of biologic and other scientific information is of tremendous import to the prestige of this nation, as it is to any nation. Despite the potential high interest of the biologist in the utilization of space exploration to accumulate knowledge on basic life processes including the origin of life itself, there is a mere handful of biologists in the United States who are thinking in terms of this aspect of our future. Responsible in part for this is the lack of realization on the part of biologists, immersed in their own research problems, of these new parameters, the opportunities afforded by the non-earth environment for the extension of understanding. In addition, from an ethical point of view, the biologist may be deterred from active participation by the enormous sums of money involved in space vehicle development. And this is an attitude undoubtedly shared by biologists and non-biologists alike. Here is an area in which the engineer can be helpful by elucidating the capabilities of projected space vehicles in order that biological experiments may be designed so as not to impose a significant additional expenditure.

Necessity for Fundamental Research

Despite certain present-day deficiencies in planning and outlook, as noted here, we may be encouraged and stimulated by the studies that are now being conducted. For this report a survey was made of biological programs related to the space effort, and many of these are briefly described below. A number of investigators, from whom information was collected concerning experimental projects underway, replied quite candidly that their work preceded interest in space exploration or was in effect work of fundamental significance with implications for space exploration only secondary. A large measure of credit must be given to NASA and to the Department of Defense who are supporting these studies. Most of these experimental programs are quite new and there are few results as yet. Of course there is another, rather more impelling reason why it is necessary to speak more of plans and purposes than of results: the fact that very little biological experimentation in space has as yet been possible.

Research Projects

Zero-gravity

Dr. Charles Lyon at Dartmouth College feels that in the plant world the fast-growing herbaceous annuals might well be found to be the most efficient producers of oxygen as well as supplementary food sources. Since each crop must be started anew from seed, the effect of gravity-free space as well as other space capsule conditions upon seedlings must be checked. He approaches this problem from the point of view that since the growth of plant tissue is quite closely controlled by the auxins, which are growth hormones, any gravitational effect upon auxin transport might play an important role. Lyon has demonstrated a marked effect of gravity on plant growth by the use of the clinostat, long used by botanists as an experimental means of obviating the effects of normal gravitational action.

From Emory University, Professor Geoffrey Bourne has submitted a project for the study of the weightless state on muscles in tank immersion experiments as well as actual zero-gravity on muscle fibres and other cells as well.

Dr. Cornelias Tobias and others at the University of California are concerned with the effects of the gravity-free state. For example, they are interested in a beetle, *Tribolium confusum*, the adult and larva of which infect

flour and grains, since it may, in a space flight situation, give some information as to the effect of weightlessness upon differentiation. In general, they wish to evaluate those aspects of physical chemistry which will influence the metabolism and proliferation of cells in a state of partial or complete weightlessness. Some of the parameters of living cells that may be altered are aerobic and anaerobic metabolism, induction of mutations, rate of proliferation, differentiation, and morphology.

Dr. Stephen W. Gray and his group at Emory University replied that the nature of their overall interest in space research was to gain basic understanding of the role of gravity in determining growth and form of tissues and cells. In conjunction with Dr. Betty F. Edwards he has published results of the effect of supranormal gravitational forces on cell division in wheat seedlings and on the swimming habits of tadpoles, and is studying the effects of these forces on chick heart muscle grown outside the body under laboratory conditions. He emphasized that the most important gravitational problem for immediate pursuit is the behavior of cells and tissues in gravitational fields less than that of the earth. Whereas high gravity may be attained experimentally, sub-normal and zero-gravity cannot, and to extrapolate from known effects in high fields to expected effects in low fields is dangerous. Long exposures to zero-gravity may be necessary; it may be that growing tissues will be affected while mature tissues will not.

Dr. Charles Wunder at State University of Iowa is primarily concerned with gravity as an environmental agent, which, although almost constant on earth, would have different intensities at other locations within our solar system. For several years he has been observing the growth of fruit fly larvae, mice, and hamsters during continual centrifugation, in order to elucidate the role of gravity in the control of growth. It has been found that continual exposure to high gravity, as simulated by centrifugation, can reduce the growth rate of fruit fly larvae. Preliminary results show that between the first and third months after birth, mice, in a continually operating centrifuge, exhibited growth inhibition at 2 g's and 5 g's and did not survive at 7 and 10 g's.

Dr. James C. Finn, Jr., at the Aerospace Laboratories, Missile Division, of North American Aviation is in the process of studying the role of constant acceleration in growth and development of higher plants, with the purpose of determining the effects of simulated zero to 2 g's on growth and development.

In 1958 Dr. H. J. Muller, an eminent geneticist, offered a system of providing a pseudo-weightless state for human beings, patterned after the clinostat, which has been mentioned as being used for obviating gravitational effects on plants. Several others simultaneously came forth with this basic idea, the nullification of gravity-orientation cues. Dr. Raphael B. Levine at Lockheed has developed a null-gravity simulator for human beings. But to reiterate, the gravity-free state can only be simulated. Such methods will give some information of very practical value for man under earth-free conditions. However, fundamental questions concerning the influence of zero-gravity on biologic processes simply cannot be answered in this way.

Radiation

The interaction of living material and various types of electro-magnetic and corpuscular radiation produces a broad spectrum of physical, chemical and biological effects which have been under study for a little more than half a century. The discoveries of Becquerel, Röntgen, and the Curies opened up whole new areas in medicine and the natural sciences. Today the destruction of both malignant and normal tissue with the use of X-rays and radioactive substances is a well-known if not fully understood phenomenon. In present day cellular biology the uses of various forms and intensities of radiation are manifold.

One of the most fascinating of these is the production of mutations by the alteration of a finite part of the self-replicating, hereditary material of the cell, the DNA. The observation of the specific effects, be they gene mutations, gross chromosomal alterations, or more extensive cellular damage, of a specific kind of radiation can provide valuable information as to the structure or function or composition of mammalian cells, bacteria, plant cells, viruses, and so forth. Such studies are of basic importance, as well as of immediate practical value to man.

Dr. Tobias and his group have for several years been studying the biological effects of heavily ionizing radiations as well as their pertinence to space flight. In addition to his gravity studies, Dr. Bourne has initiated a project for the study of the effects of the types of radiation met by high altitude rockets and satellites on the muscular function of live frogs. Dr. Franklin Hutchinson at Yale has been interested in the biological action of very heavy ions. The chief purpose has been to gain further understanding of the living cell and cellular constituents. However, since fast heavy ions are found in primary cosmic radiation, the importance of this work to space travel has become apparent. One aspect of these studies is the effect of these ions on chromosome structure detected by the production of chromosomal aberrations.

Dr. A. Gib DeBusk of Florida State University has an extensive program for research in space genetics, which involves the exposure of suitable biological systems to the Van Allen radiation belts and to solar cosmic radiation over a prolonged period of time. Very elegant genetic bioassay systems have been devised as an essential preliminary to man's entrance into these regions. Dr. DeBusk is interested in answering the question as to whether primary cosmic radiation can produce gene mutations. It is known that they cause cell death, but do they cause mutations, either in the molecular sense or as gross chromosomal changes? Of timely

interest is his report that on September 19, 1960 his biological test system, using the bread mold, *Neurospora*, was exposed to the inner Van Allen radiation belt, and that this was the first so-called biological flight. The sample was recovered, having reached an altitude of approximately 1130 miles for 26 minutes, and is undergoing genetic and physiological tests in his laboratory.

Algae and Other Plants in a Closed Ecological System

The algae have come under close scrutiny as a possible biological system for maintaining man within the closed ecological environment of the space vehicle. Although the purpose here is an eminently practical one, such studies lead to the accumulation of further basic information concerning this large and diverse group of organisms, some of which are unicellular, some of which are in aggregate form, as for example seaweeds. Moreover, great impetus has been given to the study of photosynthesis, of fundamental importance to our existence.

The algae have shown the greatest promise for on one hand acting as a photosynthetic gas exchanger and on the other as a source of food for human beings. The presence of chlorophyll permits, in simple terms, thermodynamic conversion of light energy into chemical energy, whereby CO_2 and water are reduced to carbohydrate with the liberation of oxygen. The initial product is sugar which is converted and stored as starch, upon polymerization. Other materials, such as proteins and vitamins, are formed indirectly.

Dr. Robert Krauss at the University of Maryland initiated two research programs concerned with certain aspects of the basic physiology of the algae. His group was the first to grow algae in a closed recycling system for 3 months with only inorganic nutrients. It was a critical test of the absorption rates of inorganic elements, and it contributed to the present concept of the use of algae in the closed ecological system. He is interested in the effect of the space environment at a cellular level, but points out that the studies are concerned primarily with biological phenomena of fundamental interest.

Dr. Hiroshi Tamiya of the Tokugawa Institute of Tokyo has conducted a number of studies on the use of algae, primarily *Chlorella* and *Scendesmus* which belong to the group of green algae, as food or animal feed. In 1942 several German scientists first suggested the large scale industrial production of algae as a food source. As Dr. Tamiya points out, the use of algae as food has been practiced in the Orient since ancient times, especially in Japan. Dr. Tamiya's studies have not been concerned with the use of algae in the space vehicle but rather with basic growth and nutritional problems. Properly processed *Chlorella* is non-toxic to human beings and has been found to be rich in proteins and vitamins as well as to contain carbohydrates, lipids, and minerals. Compared to animal protein its greatest drawback is its low content of one of the essential amino acids, methionine. Another interesting project is the growing of *Chlorella* with a species of *Daphnia* or water-fleas, by which it is hoped to devise an efficient system for the conversion of plant protein to animal protein.

An extensive program of biological and engineering studies is underway at the Electric Boat Division of General Dynamics for the development of a photosynthetic gas exchange system for space vehicles. The algae are being utilized, at least at present, although the plant kingdom is being surveyed in detail. A particular strain of *Chlorella*, discovered in 1953, has been selected. It is a thermophilic strain, growing and photosynthesizing optimally at 39 to 40° C. and with a tremendously increased growth rate. Heavy cell concentrations of this alga may be employed, since the requisite light sources for a maximal rate of photosynthesis can be of a very high intensity without inhibition due to light saturation. An additional project is the wide-scale screening of algae in order to find an even more efficient and practicable organism.

Dr. Robert Tischer at Mississippi State College is doing basic research on the physics, chemistry, and microbiology of closed ecological systems, in order to elucidate possible biochemical pathways from human waste products back to human food. Various kinds of microorganisms are under evaluation, for example certain bacteria, molds, yeasts, and protozoa, as possible recycling agents for the provision of nutrient for algal cultures.

At North American Aviation research is in progress to examine the possible role of the angiosperms, higher plants, in space operations. The stated purpose is to determine the optimal growth and development of certain plants in reference to gas exchange rates and food production under conditions under which all environmental factors, except magnetism and high energy radiation, are controlled.

Dr. Frank Salisbury and Dr. Ralph Baker at Colorado State University are interested in various aspects of plant growth under artificial environments. They feel that higher plants can be made to photosynthesize with greater efficiency, that they are generally more edible than the algae, that they might be useful in a water purification system, and that in any case their utilization is almost certain for future space exploration or planetary habitation. Two projects have been initiated. One is the response of certain plants and their photosynthetic rate to high light intensities as might be found on the moon, in addition to other variables such as elevated temperature and a high CO_2 atmosphere. The second project is the study of plants grown under germfree conditions, similar in concept to the animal studies which have been underway for many years. As is well known, associated with the intestinal tract of animals including human beings are various kinds of nonpathogenic bacteria. The roots of plants likewise exist in close association with a variety of bacteria, fungi,

and so forth. Their influence is considered significant, but has not been well elucidated.

Biological Rhythms

The subjection of men to alien environments wherein the familiar alternation of daylight and darkness are absent, where he is outside the earth's magnetic field, and where he might not be able to have his approximately 8 hours sleep every 24 hours, has led to a heightened interest in the many rhythmic processes in plants and animals which are, or seem to be, related to the 24 hour solar day. There has been a considerable amount of research in this area since the early '30s, chiefly in Germany and Holland as well as in this country and the United Kingdom. In broad perspective the problem is this: Are the many observable daily biological rhythms built into the organism as a sort of biological clock, or are they controlled by an external geophysical periodicity? The basic studies of such investigators as Dr. Colin S. Pittendrigh at Princeton and Dr. Frank A. Brown, Jr. at Northwestern University are of tremendous significance to space travel. In this area, likewise, Dr. Finn at North American is conducting a study concerned with this question of endogeny vs. exogeny of biological rhythms in plants, in order to determine whether diurnal fluctuations in the earth's magnetic field are responsible for the periodicity (but not the phasing) of daily biological rhythms.

Other Experimental Areas

There are many other areas of fundamental research which do not fall conveniently into the previously mentioned categories. For example, Dr. Emmett W. Chappelle at RIAS is interested in the fundamental mechanisms of carbon monoxide fixation—that is to say, the incorporation of CO gas into a compound utilizable to a living organism. There are several microorganisms which are known to be able to do this, among them the green alga *Scendesmus*. Carbon monoxide fixation may be of practical importance in closed ecological systems.

Dr. L. Joe Berry at Bryn Mawr College is concerned with the needed additional knowledge as to the response of human beings to high altitudes or lowered oxygen tension over a long period of time. It is postulated that animals carrying pathogenic organisms can become overtly diseased at lowered atmospheric pressures. The effect in mice of various combinations of altitude and oxygen concentration on tissue citric acid, carbohydrate lability, susceptibility to infection, and other physiological processes are being investigated.

Extra-terrestrial Life and the Origin of Life

This last category is of great significance to natural science as well as highly stimulating to man's imagination. But while there are a number of projected studies there is obviously little positive information with which to work. The difficulties are compounded by the fact that we do not truly know what to look for. On earth all living material has a backbone of carbon, which is derived from CO_2 and which is converted to organic matter by means of the utilization of the sun's energy during the photosynthetic process. But did the atmosphere always contain CO_2? And what happened before the highly complex chlorophyll molecule was elaborated? Then of course there is the all important question of whether there could be a self-replicating system based on an element other than carbon, and whether we would recognize it as a "living" system.

There are at present several closely related active programs. Since it is highly possible that under suitable conditions, life might have arisen independently on other planets, recommendation has been made by the International Committee on Contamination by Extra-terrestrial Exploration that space vehicles be sterilized in order to avoid contamination of the moon and other planets. In this way confusion of results from life detection systems as well as possible harmful effects of the organisms themselves in an alien environment can be avoided. We know that the Russian moon probe was reportedly sterilized. In the United States there are rigorous sterilization procedures and active programs for their further development. This is in itself a difficult task and necessitates the close collaboration of biologist and engineer. Dr. Joshua Lederberg, the Nobel Prize winning microbiologist at Stanford University, has concerned himself with this problem, especially in relation to his plans for a cytochemical study of extra-terrestrial organisms by the use of a vidicon microscope for telemetered observation. Elsewhere other detection systems are being developed which involve, for example, the examination of planetary materials, or the analysis of planetary reflection spectra.

Conclusion

It was hoped that some suggested requirements, in engineering terms, for conducting biological experiments in space, could be reported. Though this question was posed specifically to investigators in the course of collecting information on present biological experiments, actually only two replies were volunteered. Perhaps the reason this was so has already been brought out and can well be reiterated here in summarizing.

The development of a particular crossbreed of life scientist and engineer specifically for the design or performance of extraterrestrial biological experiments, as well as for manned space flight, may be undesirable in an age of needed specialization. However, until this interdisciplinary capability becomes the general case, rather than exhibiting itself in only a few especially talented and motivated individuals, we are under an imperative demand. The communication barriers between the biologist and engineer, or generally between the life scientists on one side and on the other those designing space vehicles and planning space missions, must be broken down.

The efforts of independent organizations such as the American Astronautical Society; the support being given by the Department of Defense to attracting the interest of biologists; the creation of the NASA Life Sciences Division and the drafting of its 10 year projected program are all so guided. However, recognition of the problem and educational effort exerted not only through the public news media but also through the particular journals, or reviews, read by biologists and engineers may accelerate the kind of thinking which speeds up lead times in experimental concept and design. The widespread dissemination of even preliminary results will stimulate both thought and action. Furthermore, international cooperation, the blending of our engineering capability with the very real and creative abilities of scientists of other countries, would be unmeasurably productive to biological and medical science, as well as contributory to understanding between peoples.

Two specific points have been advanced in this report by which the engineers and the physical scientists could be guided in these space age endeavors. One is that biological science is still in a comparatively early developmental stage. The other is that a clear grasp is needed of those areas of space flight which require biologists to be an integral part of the earliest planning team, so that the necessary lead time is provided for observation, experimentation, and study, that space exploration can progress in an orderly, scientific fashion without grave and unnecessary stumbling blocks.

In conclusion, it is suggested that man's role as observer and monitor receive frequent and penetrating re-evaluation. From the descriptions given here of what are the very early space researches conceived by scientists, it is a short step to imagining the vast possibilities of future scientific experimentation in space or planetary environments. And it is hoped, from this brief exposition, that there is increased awareness of the very real advances that are being made right now as well as the tremendous potential that is offered for the furtherance of basic biological knowledge.

Acknowledgment

Grateful acknowledgment is made to the investigators whose studies are cited in this report.

References

1. Report of the Senate Committee on Aeronautical and Space Sciences, "Space Research in the Life Sciences: An Inventory of Related Programs, Resources, and Facilities," 86th Congress, 2nd Session.
2. Science Information Exchange (selected project reports). Supporting agencies of SIE include Atomic Energy Commission, Department of Defense, National Aeronautics and Space Administration, National Science Foundation, Public Health Service, Veterans Administration.
3. "Physics and Medicine of the Atmosphere and Space" held at San Antonio, Texas, November 10 and 11, 1958; sponsored by the School of Aviation Medicine, Aerospace Medical Center, Brooks Air Force Base, Texas; editors, Otis O. Benson, Jr. and Hubertus Strughold.
4. "Space Research," proceedings of the 1st International Space Symposium, Nice, France, 1960; Editor, H.K.K. Bijl; Publisher, North Holland Publishing Company, Amsterdam. (Available U.S. Interscience Publishers, Inc., New York City.)
5. ARDC-TR-58-58, ASTIA Document No. Ad204 761, "Biological Payloads in Space Flight," 2–5 September 1958, sponsored by Air Research and Development Command Headquarters, Contract AF 18 (600)-1792, Division of Educational Research, University of Virginia, Charlottesville, Virginia.

The Orbital Motion of Pellet Clouds[1]

Stanley Ross[2]

Abstract

The motion of a cloud of pellets is analyzed following their sudden release from a spinning container. The incremental velocities imparted by the spin motion are interpreted as time integrals of impulsive perturbation accelerations which modify the parameters of the container's orbit. By transforming these orbit element changes into linear displacements, the subsequent cloud shape may be studied analytically. Some examples are included which illustrate the results for certain special cases.

[1] Manuscript submitted January 12, 1961.

[2] Research Scientist, Lockheed Missiles and Space Company Palo Alto, Calif.

Symbols

At the instant of pellet release:

Symbol	*Definition*
ϕ	particle angular position in the container
$\dot{\phi}$	spin velocity of the container
$\mathbf{p}$	particle vectorial position, measured from some fixed point on the spin axis
$\mathbf{V} =$	$\dot{\phi} \times \mathbf{p}$
α	yaw angle of container, measured positively to starboard
β	pitch angle of container, measured positively upward

For the container's orbit:

$\Omega, i, a, e, n, \epsilon, \omega$ are orbital parameters, as defined in Ref. (1).

v instantaneous true anomaly

$u = v + \omega$

$h = e \sin \omega$
$l = e \cos \omega$
$\hat{\mathbf{R}}, \hat{\mathbf{S}}, \hat{\mathbf{W}}$, are unit perturbing accelerations, directed radially outward, circumferentially forward and orthogonally upwards, as defined in Ref. (1), page 402.
T time, measured from instant of explosion
dx, dy, dz are rotations measured about orthogonal reference axes.

$$K = \frac{p\dot{\phi}}{na}$$

Introduction

One means of creating an orbiting aggregate of individual particles is to suddenly burst a spinning shell packed with small pellets. The freed particles, each experiencing an additional velocity component imparted from the spin motion, separate to form a cloud which continues to circle the Earth.

Suppose the angular velocity of the casing is specified by the vector $\dot{\boldsymbol{\phi}}$; then a particle which occupies a position $\mathbf{p}$ measured from some fixed point on the spin axis acquires an incremental velocity $\mathbf{V} = \dot{\boldsymbol{\phi}} \times \mathbf{p}$. The motion of each pellet prior to the shell explosion is described by the orbital parameters common to the aggregate, e.g., Ω, i, a, h, l, ϵ.[3] Removal of the container produces changes in the orbit of each particle which may be characterized by the familiar equations of variation of the elements. If the rupture is assumed to occur instantaneously, the "perturbing accelerations" may be treated as impulse functions whose time integrals are merely the appropriate incremental velocity components. The orbital elements then change in accordance with the following relations:[4]

$$d\Omega = \left[\frac{r \sin u}{na^2\sqrt{1 - e^2} \sin i}\right]_0 (\mathbf{V}\cdot\hat{\mathbf{W}}),$$

$$di = \left[\frac{r \cos u}{na^2\sqrt{1 - e^2}}\right]_0 (\mathbf{V}\cdot\hat{\mathbf{W}}), \tag{1}$$

$$da = \left[\frac{2e \sin v}{n\sqrt{1 - e^2}}\right]_0 (\mathbf{V}\cdot\hat{\mathbf{R}}) + \left[\frac{2a\sqrt{1 - e^2}}{nr}\right]_0 (\mathbf{V}\cdot\hat{\mathbf{S}}),$$

$$dh = -\left[\frac{\sqrt{1 - e^2} \cos u}{na}\right]_0 (\mathbf{V}\cdot\hat{\mathbf{R}}) + \left\{\left[\frac{2\sqrt{1 - e^2} \sin u}{na}\right]_0 - \left[\frac{r\sqrt{1 - e^2}\, e}{na^2(1 - e^2)} \cos u \sin v\right]_0\right\} (\mathbf{V}\cdot\hat{\mathbf{S}}) - \left[\frac{re \sin u \cos \omega}{na^2\sqrt{1 - e^2} \tan i}\right]_0 (\mathbf{V}\cdot\hat{\mathbf{W}}),$$

$$dl = \left[\frac{\sqrt{1 - e^2} \sin u}{na}\right]_0 (\mathbf{V}\cdot\hat{\mathbf{R}}) + \left\{\left[\frac{2\sqrt{1 - e^2} \cos u}{na}\right]_0 + \left[\frac{r\sqrt{1 - e^2}\, e}{na^2(1 - e^2)} \sin u \sin v\right]_0\right\} (\mathbf{V}\cdot\hat{\mathbf{S}}) + \left[\frac{re \sin u \cos \omega}{na^2\sqrt{1 - e^2} \tan i}\right]_0 (\mathbf{V}\cdot\hat{\mathbf{W}}),$$

[3] Anticipating that shell orbit eccentricities will be small for many problems of practical interest, we have chosen the variables h, l, ϵ to specify the orbit in view of their analytic behavior near $e = 0$. That is, $h = e \sin \omega$, $l = e \cos \omega$, $\epsilon = \pi - \sigma$ (Ref. 1, pp. 406 and 421).

[4] We assume that K, the ratio of incremental speed to orbital speed, is small.

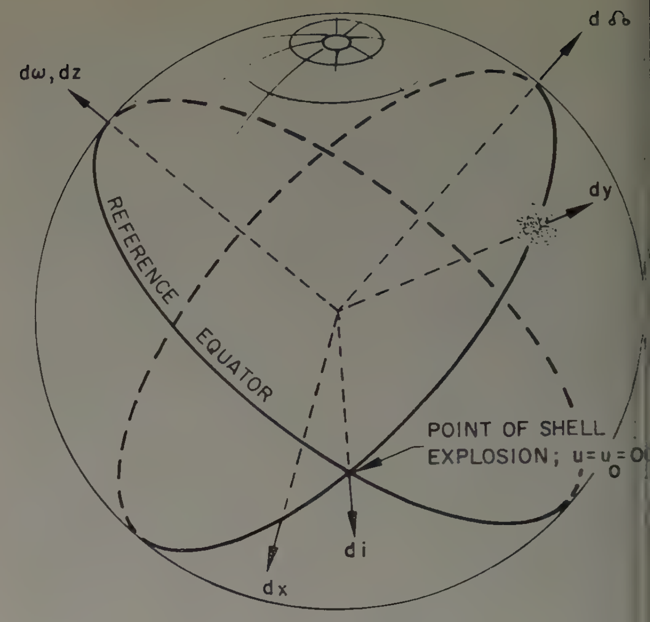

FIG. 1. Resolution of element perturbations

and

$$d\epsilon = \left\{\frac{-1}{na^2}\left[2r + \frac{a\sqrt{1 - e^2}}{e}(1 - \sqrt{1 - e^2}) \cos v\right]_0\right\} \cdot(\mathbf{V}\cdot\hat{\mathbf{R}}) + \left[\frac{\sqrt{1 - e^2}}{nae} \sin v\left(1 + \frac{r}{p}\right)(1 - \sqrt{1 - e^2})\right. \cdot(\mathbf{V}\cdot\hat{\mathbf{S}}) + \left[\frac{r \sin u \tan \frac{i}{2}}{an^2\sqrt{1 - e^2}}\right]_0$$

In Eq. (1), $\hat{\mathbf{R}}$, $\hat{\mathbf{S}}$, $\hat{\mathbf{W}}$ and are unit vectors in the radial, circumferential, and orthogonal direction (Ref. 1, p. 402), while the other quantities on the righ sides of Eq. (1) (the symbols are those of Ref. 1 are evaluated at the moment of explosion.

Since we are examining two-body motion about spherical Earth, there is no physically preferred direc tion in space. Therefore, any coordinate system ma be chosen which will simplify the analysis. If a referenc equator is established orthogonal to the shell's orbi and passing through the position of the explosion (se Fig. 1), then $d\Omega$, di, and $d\omega$ may be transformed int small rotations dx, dy, and dz about the axes shown:

$$dx = -\cos u \, d\Omega + \sin u \, di,$$

$$dy = \sin u \, d\Omega + \cos u \, di, \tag{2}$$

and

$$dz = d\omega.$$

Also, since

$$r = \frac{a(1 - e^2)}{1 + e \cos(u - \omega)},$$

the radial displacement at any time t may be expressed as:

$$dr = \left(\frac{\partial r}{\partial a}\right)_t da + \left(\frac{\partial r}{\partial e}\right)_t de + \left(\frac{\partial r}{\partial \omega}\right)_t d\omega. \quad (3)$$

Finally, by adopting the formula in Ref. 1, p. 171, and from the definitions of h and l (n.b., $u_0 = 0$), it can be shown that

$$n(t - t_0) = u - 2\,[l \sin u - h(\cos u - 1)] + \cdots \quad (4)$$

where t_0 is the time of explosion. For $T = t - t_0$, therefore, the angular gain in particle position along the orbit is given by

$$dz + du = d\omega$$

$$+ \frac{2[dl \sin u - dh(\cos u - 1)] - \dfrac{3n}{2a} T\, da}{1 - 2(l \cos u + h \sin u)}. \quad (5)$$

Thus, at any time after the release of the pellets, the positional change of each particle may be closely approximated by the following expressions:

$$dR = dr,$$

$$dS = r[dz + du], \quad (6)$$

and

$$dW = r\, dx.$$

Initial Orbits Circular

When the orbit of the container is circular, $de = \sqrt{dh^2 + dl^2}$, and $d\omega = 0$, from the definitions of h and l. Consider a cylindrical shell, travelling on a circular orbit, whose (longitudinal) spin axis at the moment of explosion is yawed to starboard by α degrees, and pitched upwards by β. Here we have:

$$\mathbf{V}\cdot\hat{\mathbf{R}} = -p\dot{\phi}[\cos\alpha \cos\phi + \sin\alpha \sin\phi \sin\beta],$$

$$\mathbf{V}\cdot\hat{\mathbf{S}} = p\dot{\phi}[\sin\alpha \cos\phi - \cos\alpha \sin\phi \sin\beta],$$

and

$$\mathbf{V}\cdot\hat{\mathbf{W}} = p\dot{\phi}[\cos\beta \sin\phi + \tfrac{1}{4}\sin 2\alpha \sin 2\beta \cos\phi].$$

The eference direction $\phi = 0$ lies in the plane formed by $\hat{\mathbf{W}}$ and $\dot{\boldsymbol{\phi}}$ when the cloud is released. It is perpendicular to $\dot{\boldsymbol{\phi}}$, and points away from $\hat{\mathbf{W}}$, as in Fig. 2. Denoting by K the ratio of incremental speed to circular speed,

$$K = \frac{p\dot{\phi}}{na},$$

we suppose $K^2 \ll K$. Then, from Eq. (1), since $u_0 = 0$; $i_0 = \dfrac{\pi}{2}$:

$$d\Omega = 0,$$

$$di = K[\cos\beta \sin\phi + \tfrac{1}{4}\sin 2\alpha \sin 2\beta \cos\phi],$$

$$da = 2aK[\sin\alpha \cos\phi - \cos\alpha \sin\phi \sin\beta],$$

$$dh = K[\cos\alpha \cos\phi + \sin\alpha \sin\phi \sin\beta],$$

and

$$dl = 2K[\sin\alpha \cos\phi - \cos\alpha \sin\phi \sin\beta];$$

and, consequently,

$$de^2 = K^2[\cos\alpha \cos\phi + \sin\alpha \sin\phi \sin\beta]^2 + 4K^2[\sin\alpha \cos\phi - \cos\alpha \sin\phi \sin\beta]^2.$$

By Eq. (2),

$$dx = K[\cos\beta \sin\phi + \tfrac{1}{4}\sin 2\alpha \sin 2\beta \cos\phi] \sin u$$

and

$$dz = 0.$$

From Eq. (3),

$$dr = da - a\cos(u - \omega)de + \vartheta(K^2)\cdots,$$

where

$$\omega = \tan^{-1}\left(\frac{dh}{dl}\right).$$

Substituting the proper expressions for da and de, we find that dr becomes:

$$dr = da[1 - \sec\omega \cos(u - \omega)].$$

Finally, we have from Eq. (6), to first order in K:

$$dR = 2aK[\sin\alpha \cos\phi - \cos\alpha \sin\phi \sin\beta] \cdot[1 - \sec\omega \cos(nT - \omega)],$$

$$dS = aK[\sin\alpha \cos\phi - \cos\alpha \sin\phi \sin\beta] \cdot[-3nT + 4\sec\omega \sin(nT - \omega) + 4\tan\omega], \quad (7)$$

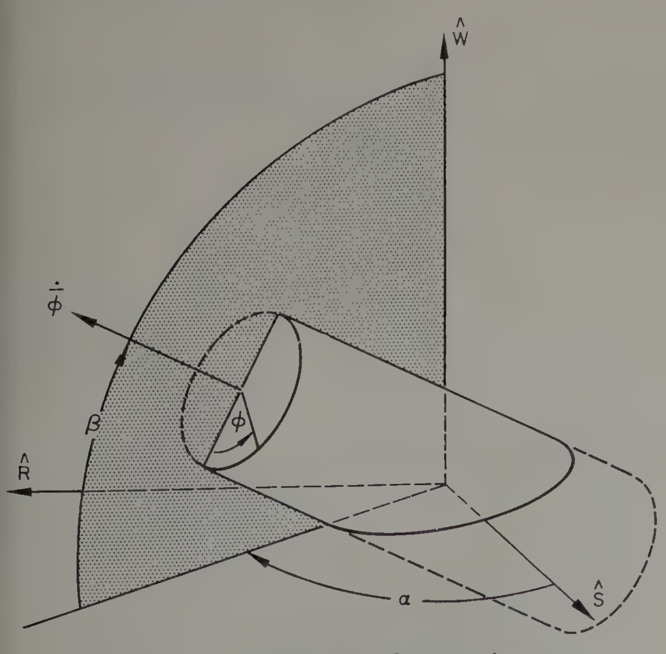

Fig. 2. Nomenclature and conventions

and

$$dW = aK[\cos\beta \sin\phi + \tfrac{1}{4}\sin 2\alpha \sin 2\beta \cos\phi] \sin nT.$$

Since α and β are independent and arbitrary, it follows that the secular term in dS vanishes when and only when $\alpha = \beta = 0$.

Some Examples

By setting the eccentricity of the shell's orbit equal to zero, we are free to examine several interesting examples unencumbered by complex initial orbit parameter effects. Three special cases illustrate the physical features of clouds which result from initial spin alignments purely in the $\hat{\mathbf{S}}$, $\hat{\mathbf{W}}$, and $\hat{\mathbf{R}}$ directions.

Case I. The spin axis is aligned with the velocity vector when the cloud is released. Then $\alpha = \beta = 0$, $\omega = \pm\pi/2$, and Eq. (7) becomes:

$$dR = -aK \cos\phi \sin nT,$$

$$dS = 2aK \cos\phi[1 - \cos nT],$$

and

$$dW = aK \sin\phi \sin nT.$$

Squaring and adding terms, we find

$$(dR)^2 + (dW)^2 = (aK \sin nT)^2$$

and

$$\frac{dW}{dR} = -\tan\phi.$$

Each particle harmonically traces a straight line in the **R**, **W** plane (Fig. 3), and the cloud itself becomes a radially pulsating cylinder, slowly oscillating about its longitudinal axis, with its end-faces tilting sinusoidally with time (Fig. 3).

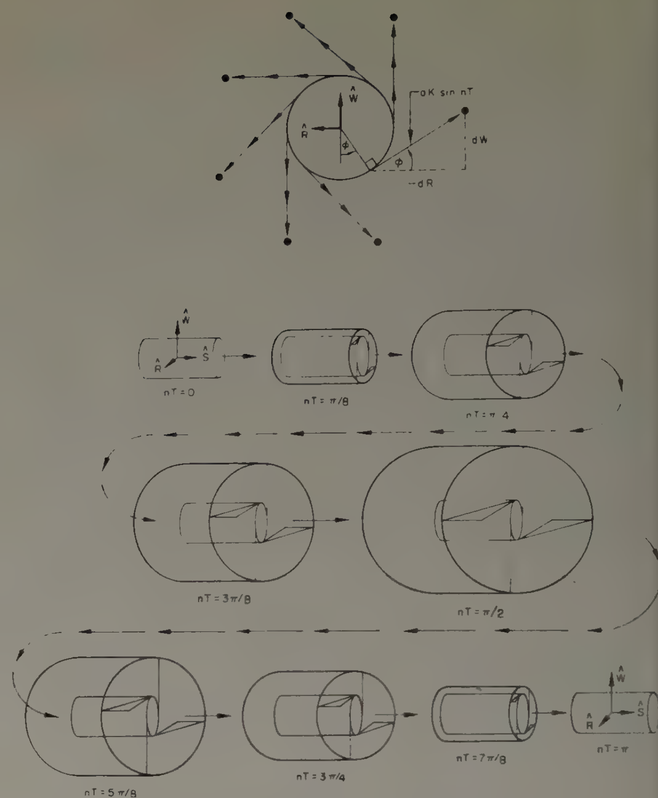

FIG. 3. Pellet cloud history. Spin axis aimed forward at $T = 0$

Qualitatively speaking, the properties of this cloud are governed by the fact that the incremental velocity vector applied to each pellet has components in the $\hat{\mathbf{W}}$ and $\hat{\mathbf{R}}$ directions only. The contribution along $\hat{\mathbf{W}}$ merely changes the inclination of the particle orbit, while the R-impulse modifies the eccentricity, but not the period, since an impulse applied normal to the

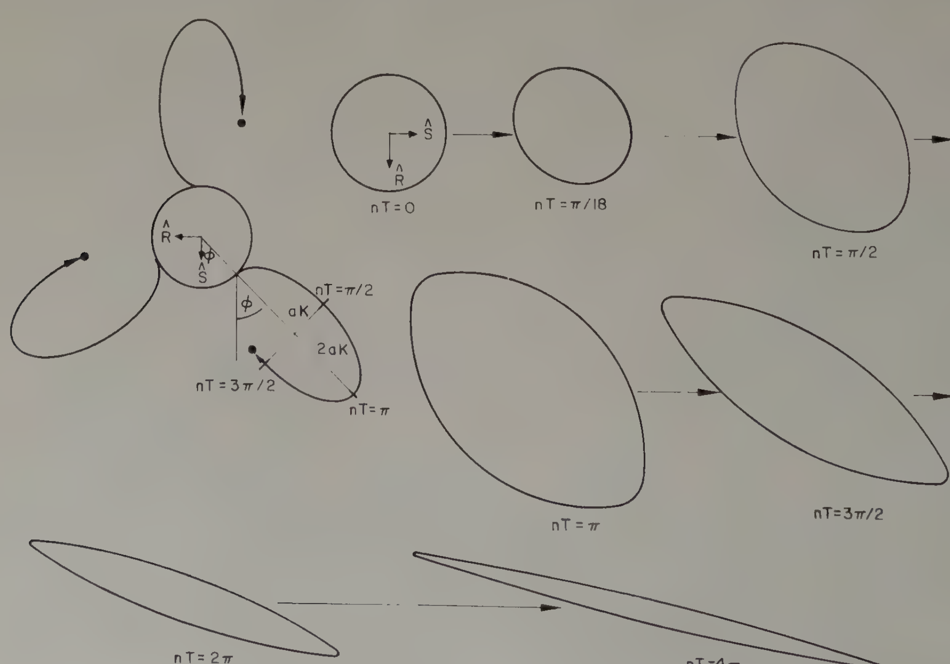

FIG. 4. Pellet cloud history. Spin axis aimed upward at $T = 0$

velocity vector leaves the energy, and therefore the period, unchanged. The combined perturbations are thus strictly periodic.

Particles for which the R-impulse is directed inwards (i.e., $-\pi/2 < \phi < +\pi/2$) find themselves at the latus rectum of the new orbit, travelling towards perigee; these move somewhat faster than nominally at first. Particles subjected to an outward-directed R-impulse ($\pi/2 < \phi < 3\pi/2$) move more slowly at first. Hence the exhibited periodic variation in the end-face slope of the cloud.

Case II. When the spin axis is aimed northwards at $T = 0$, then $\alpha = 0$, $\beta = \pi/2$, and $\tan \omega = -\frac{1}{2} \cot \phi$. Again from Eq. (7):

$$dR = aK[2 \sin \phi (\cos nT - 1) - \cos \phi \sin nT],$$

$$dS = aK[-\sin \phi \sin nT - 2 \cos \phi (\cos nT - 1)] + 3aK \sin \phi (nT - \sin nT),$$

and

$$dW = 0.$$

Since $dW = 0$, there are no pellet plane changes, and the cloud cannot expand in height. This time, however, the spin motion also adds incremental speeds in the tangential direction. The energies are altered, and the cloud loses its property of periodicity. For particles located at $\phi = \pi/2$ and $\phi = -\pi/2$, the motions are purely forward, and the pellets enter into their new orbits at apogee and perigee, respectively.

Except for the secular term $3aK \sin \phi (nT - \sin nT)$ appearing in dS, the figure traced by each pellet would be an ellipse with axes of length $2aK$, $4aK$; the major axis of each ellipse is an extension of $\mathbf{R}_0$, the particle's initial radial position from the spin axis (Fig. 4).

Ordinarily, therefore, the cloud shape would be not unlike the pulsating cylinder of Case I, but the secular term in this case superimposes a relative drift upon the motion of each pellet, so that the cylinder eventually dissipates itself into a smear along the orbit. Figure 4 traces this development, starting from $T = 0$.

Case III. For a radially (outward) directed spin axis, $\alpha = \pi/2$, $\beta = 0$, and $\omega = 0$, or π. Here,

$$dR = 2aK \cos \phi [1 - \cos nT],$$

$$dS = aK \cos \phi \sin nT - 3aK \cos \phi [nT - \sin nT],$$

and

$$dW = aK \sin \phi \sin nT.$$

By analysis similar to the above, the cloud shape here exhibits the cylindrically pulsating, oscillatory behavior discussed in Case I, coupled with a rectilinear drift of the type mentioned in Case II.

Acknowledgments

The author wishes to express his sincere appreciation to Frank W. McNolty and Dr. John V. Breakwell of Lockheed Missiles and Space Company for advice helpfully supplied during the course of a number of informal discussions.

References

1. Moulton, F. R., *An Introduction to Celestial Mechanics*, 2nd ed., New York, MacMillan, 1958.

Estimation of Longitudinal Variations in the Earth's Gravitational Field From Minitrack Observations[1]

W. M. Kaula[2]

Abstract

A term in the Earth's gravitational field

$$V_{nm} = \frac{kM}{r} (J_{nm} \cos m\lambda + K_{nm} \sin m\lambda) \left(\frac{R}{r}\right)^n P_{nm}(\sin \phi)$$

will cause a satellite to vary in its orbit with a frequency (0 or 1)$\dot{\omega} + m(\dot{\Omega} - \dot{\theta})$, where $\dot{\omega}, \dot{\Omega}$, and $\dot{\theta}$ are the frequencies of rotation of the perigee, the node, and the earth respectively. Estimates of the magnitudes of the J_{mn}, K_{mn} based on terrestrial gravimetry indicate that some of these orbital variations will be of about ± 100 meters in amplitude.

Investigation of other causes of residuals in satellite observations—other orbital variations, electronic environmental and instrumental effects, orbital computation methods, geodetic datum error—indicates that none of them will give rise to exactly the same spectrum of variations in the residuals as the gravitational harmonics. Hence the gravitational terms should be determinable from observations of adequate distribution and number.

In the case of Minitrack observations of a single satellite, limitation of observations to high altitudes on the meridian makes it difficult to distinguish one gravitational term from another except through the difference in phase shift of the

[1] Submitted March 27, 1961.

[2] Goddard Space Flight Center, National Aeronautics and Space Administration.

spectrum for different stations. Hence the attempt to estimate the gravitational terms must be made simultaneously with the data from all stations. The results obtained from 3077 observations of the Vanguard I satellite are as follows:

$$J_{22} = -0.69\ (\pm 1.2) \times 10^{-6},$$
$$J_{41} = -1.02\ (\pm 0.35) \times 10^{-6},$$
$$K_{22} = +1.17\ (\pm 1.2) \times 10^{-6}$$

and

$$K_{41} = +0.30\ (\pm 0.35) \times 10^{-6}.$$

The principal defect in these results is probably systematic error in the orientations of the Minitrack antennas.

Introduction

The Earth's gravitational potential may be represented as a sum of spherical harmonics:

$$V = -\frac{kM}{r}\left[1 - J_{20}\left(\frac{R}{r}\right)^2 P_{20}(\sin\phi) - \sum_{n,m}(J_{nm}\cos m\lambda + K_{nm}\sin m\lambda)\left(\frac{R}{r}\right)^n P_{nm}(\sin\phi)\right], \quad (1)$$

in which kM = gravitational constant $\times$ earth's mass, r = radius vector, ϕ = latitude, λ = longitude, R = Earth's radius, $P_{nm}(\sin\phi)$ is a Legendre Associated Function, and the J's and K's are independent coefficients. J_{n0} is usually written as J_n, and $K_{n0} = 0$ since $\sin 0 = 0$.

$J_{20} = 1.0823\ (\pm .0003) \times 10^{-3}$, the term due to the Earth's oblateness, has been estimated now many times from secular changes of satellite orbits. Estimates have also been made of J_{n0} for $n = 3$ through 6, that of $J_{30} = -2.3\ (\pm 0.1) \times 10^{-6}$ in particular being well confirmed (Refs. 1–4).

However, in addition to these five J_{n0}'s which have been estimated, there exist 38 other coefficients J_{nm}, K_{nm}, $m \neq 0$, $n \leqq 6$, which express longitudinal variations in the gravitational field, and which are of just as great an interest to geophysicists. Existing terrestrial gravimetry indicates that the order of magnitude of these J_{nm}, K_{nm} will be the same as that already determined for the J_{n0}: about 10^{-6} for normalized spherical harmonics. The terrestrial gravimetry is not distributed well enough, however, to give a reliable determination of any individual harmonic J_{nm} or K_{nm}. Hence our purpose is to investigate whether it is feasible to estimate any of the longitudinal harmonics from satellite motions, and, if so, how.

The expression in Eq. (1) of the gravitational potential can be transformed from r, ϕ, λ coordinates to osculating elements' $(a, e, i, \Omega, \omega, M)$ coordinates by some more or less tedious algebra (Ref. 5), i.e.,

$$V = -\frac{kM}{a}\left[\sum_{q=-\infty}^{\infty} G_{0q}(e)\cos qM - J_{20}\left(\frac{R}{a}\right)^2 \cdot \sum_{p=0}^{2} F_{20p}(i) \sum_{q=-\infty}^{\infty} G_{20q}(e) S_{20pq}(\omega, M) - \sum_{n=2}^{\infty}\left(\frac{R}{a}\right)^n \sum_{m,p=0}^{n} F_{nmp}(i) \sum_{q=-\infty}^{\infty} G_{npq}(e) \cdot S_{nmpq}(\omega, m, \theta, \Omega)\right], \quad (2)$$

where

$$S_{nmpq} = \begin{Bmatrix} J_{nm} \\ -K_{nm} \end{Bmatrix}_{(n-m)\,\mathrm{odd}}^{(n-m)\,\mathrm{even}} \cos\{(n-2p)\omega + (n-2p+q)M + m(\Omega-\theta)\} + \begin{Bmatrix} K_{nm} \\ J_{nm} \end{Bmatrix}_{(n-m)\,\mathrm{odd}}^{(n-m)\,\mathrm{even}} \sin\{(n-2p)\omega + (n-2p+q)M + m(\Omega-\theta)\} \quad (3)$$

and a = semi major axis, e = eccentricity, i = inclination, ω = argument of perigee, M = mean anomaly, and Ω = longitude of the node of the osculating orbit; θ is Greenwich sidereal time; and $F_{nmp}(i)$ and $G_{npq}(e)$ are polynomials in the inclination and eccentricity, respectively.

The first term in V causes the unperturbed elliptical orbit. The most prominent effects of the J_{20} term are the secular changes in the node, $\dot{\Omega}$, and in perigee, $\dot{\omega}$. Since J_{20}^2 is of the same order of magnitude as the J_{nm}, K_{nm}, any attempt to deduce the latter from their first order effects on an orbit must measure such effects with reference to a computed orbit which takes into account J_{20} at least to the second order, i.e., terms containing J_{20}^2. In the present study, we used as such a reference orbit the Hansen-type numerical general orbit developed by Musen (Ref. 6).

The first order effects of the higher order coefficients J_{nm}, K_{nm} on the orbital elements can then be deduced by using the corresponding terms in V (with change of sign) as the disturbing function in the Lagrangian equations for variation of elements (Ref. 7) and integrating with respect to time. We then obtain, for example, for the perturbation of the node by a particular pair J_{nm}, K_{nm}:

$$\Delta\Omega_{nm} = \frac{1}{\dot{M}_q^{\,n+3}\sqrt{1-e^2}\sin i}\sum_{p,q}\frac{dF_{nmp}}{di} \cdot G_{npq}\int S_{nmpq}\,dt, \quad (4)$$

where $\dot{M}$ is the mean motion. On performing the integration with respect to time, $\int S_{nmpq}\,dt$, there appears in the denominator a factor

$$[(n-2p)\dot{\omega} + (n-2p+q)\dot{M} + m(\dot{\Omega} - \dot{\theta})].$$

If we take the unit of time such that $\dot{M} = 1$ then, for example, for Vanguard I $\dot{\omega} = 0.00181$, $\dot{\Omega} = -0.00124$, and $\dot{\theta} = 0.0932$. Since these terms appear in the denominator, setting $n - 2p + q = 0$ amplifies the effect by $10/m$; if further $m = 0$, the effect is either amplified by about 500 (n odd) or it is a secular perturbation (n even). As has been mentioned, this "cream" of small n, $m = 0$, $n - 2p + q = 0$ has already been skimmed off, so we must turn our attention to the possibilities of m small, $n - 2p + q = 0$: to begin with $m = 1$.

G_{npq} is of $O(e^{|q|})$, and for n odd, $q \neq 0$ for $n - 2p + q = 0$: hence the longitudinal terms of greatest effect probably have n even. J_{21}, K_{21} cannot exist, since the

Earth must rotate about an axis of maximum moment of inertia; hence the coefficients most likely to be effective are J_{41}, K_{41}. Taking estimates of the magnitude of these coefficients based on autocovariance analysis of terrestrial gravimetry (Ref. 8), we obtain as estimates of the magnitude of effect of J_{41}, K_{41} on Vanguard I about ± 200 meters. Most of this effect is in the perigee argument and mean anomaly—along the orbit; but in this respect we benefit from sole advantage of the short period over the long period analysis: the drag effects of high frequency are negligible at altitudes in excess of 500 km.

Other effects estimated from the terrestrial statistical data are J_{22}, K_{22} : ± 100 m.; J_{31}, K_{31} : ± 100 m; J_{42}, K_{42} : ± 100 m; J_{61}, K_{61} : ± 50 m. (Ref. 5).

From expressions such as Eq. (4) we can set up a $6 \times k$ matrix for the partial derivatives of the osculating elements with respect to k of the gravitational coefficients J_{nm}, K_{nm}:

$$C_{EG} = \frac{\partial(El_{osc})}{\partial(J_{nm}, K_{nm})}. \tag{5}$$

By applying the appropriate rotations, we can obtain the position vector $\mathbf{X}$ of the satellite in a coordinate system referred to the Earth's axis and the vernal equinox from the vector $\mathbf{Q}$ referred to the orbit:

$$\mathbf{X} = R_3(-\Omega)R_1(-i)R_3(-\omega)\mathbf{Q},$$

$$\mathbf{Q} = \begin{Bmatrix} a(\cos E - e) \\ a\sqrt{1 - e^2}\sin E \\ 0 \end{Bmatrix}. \tag{6}$$

The index indicates the axis for a rotation matrix and the argument indicates the angle rotated, with + for a counterclockwise rotation. By differentating Eq. (6) we obtain the partial derivatives of the components of $\mathbf{X}$ with respect to the osculating elements:

$$C_{XE} = \frac{\partial(x, y, z)}{\partial El_{osc}}. \tag{7}$$

Rotating angle θ about the z axis from the vernal equinox to the Greenwich meridian and subtracting the rectangular geodetic coordinates U_0 of an observing station gives the satellite position in a geodetic system referred to the station. Applying further rotations gives the satellite position referred to axes peculiar to an instrument at the station; for example for a radio interferometric system with east-west and north-south baselines:

$$\begin{aligned} L &= R_3\left(\frac{\pi}{2}\right) R_2\left(\frac{\pi}{2} - \phi\right) R_3(\lambda)\ [R_3(T)X - U_0] \\ &= R_{LU}[R_3(T)X - U_0]. \end{aligned} \tag{8}$$

To obtain finally the actual observed quantities one more matrix N must be applied to L; for the direction cosines l, m with respect to the E-W, N-S baselines,

$$\mathbf{N}_{lL} = \begin{Bmatrix} \frac{1}{\rho}, 0, 0 \\ 0\ \frac{1}{\rho}, 0 \end{Bmatrix} \tag{9}$$

where ρ is the range from the station to the satellite. Differentiating Eq. (9) with respect to the elements of L and combining it with Eqs. (5), (7), and (8) we obtain an observation equation relating corrections to the direction cosines l, m to corrections to the station position and to the gravitational coefficients:

$$\begin{aligned} &\mathbf{N}'_{lL} R_3\left(\frac{\pi}{2}\right) R_2\left(\frac{\pi}{2} - \phi\right) R_3(\lambda) \\ &\cdot\left[R_3(\theta) C_{XE}(\Omega, i, \omega, M) C_{EG} \begin{Bmatrix} Jnm \\ Knm \end{Bmatrix} - dU_0 \right] - d\begin{Bmatrix} l \\ m \end{Bmatrix}_{\text{OBS}} \\ &= \begin{Bmatrix} l \\ m \end{Bmatrix}_{\text{OBS}} - \begin{Bmatrix} l \\ m \end{Bmatrix}_{\text{COMP}}, \end{aligned} \tag{10}$$

where we have indicated the angular arguments in C_{XE}.

The foregoing analysis was originally made in anticipation of a proposed geodetic satellite to be observed several times a day with effective accuracies on the order of ± 30 meters, from which several gravitational coefficients should be deducible. What we actually have in hand are Minitrack observations of about ± 1 mil residuals—or an effective accuracy on the order of ± 1000 meters. About 6000 of these observations on Vanguard I have been accumulated over almost three years, so if the ± 1000 m. errors were perfectly random, we could get good estimates of several of the J_{nm}, K_{nm}.

However, the errors are not, of course, random, so we must inquire into what is the probable spectrum of the errors and how much does this spectrum overlap or alias the spectrum of effects of the gravitational coefficients J_{nm}, K_{nm} we are attempting to estimate. We can sort the possible sources of error into six classes according to the sequence of events from the original motions of the satellite in its orbit to our estimation of the J_{nm}, K_{nm}: (1) Variations of the satellite in the orbit due to physical effects not fully allowed for, such as drag, radiation pressure, tidal effects, and gravitational coefficients not included; (2) Variations of the satellite-to-station path of the radio signal from that assumed, due to irregularities of ionospheric and tropospheric refraction; (3) Geometrical limitations on the time and place of observation; (4) Tracking station position or orientation error; (5) Variations in the internal workings of the Minitrack instrumentation; and (6) Variations of the computed direction cosines due to the procedures used in the orbit computation, such as switching to a new set of reference elements each week, neglecting rotation of the orbit in differential corrections, etc. Each of these possible sources is most easily visualized in a particular coordinate system, to which our observation equation (10) or vector equation (8) can be transformed by application of the appropriate rotation matrices.

Classes (1) and (6) are most conveniently examined in terms of the orbital elements. As we have discussed,

the orbital variations on which estimation of J_{nm}, U_{nm} depends are primarily those of frequencies $m(\dot{\Omega} - \dot{\theta})$ for n even; $\pm 2\dot{\omega} + m(\Omega - \dot{\theta})$ frequencies have coefficients of $O(e^2)$. In the particular case of Vanguard I and $nm = 41$, the primary frequency is 1.014 cycles/day, while the side frequencies are 0.976 and 1.052 cycles/day. Exactly the same frequencies will arise from $nm = 61$, 81, etc. Although the amplitudes of effects on different orbital elements of one satellite will differ, a simultaneous least squares solution for all these coefficients from one satellite is impractical because the non-uniform distribution of observations makes the separation of these effects weak. Slightly different frequencies of 0.995 and 1.033 cycles/day will arise from $nm = 31$, 51, etc., with coefficients of $O(e)$. $1/(1.014–0.995) = 53$ days, so the effects should be easily separable with the available data.

There are a host of gravitationally caused variations in the orbit of frequency $\dot{M} = 10.7$ cycles/day (increasing 0.015 cycles/day/year), 21.4 cycles/day, 32.1 cycles/day, etc. with total amplitude less than ± 100 meters (Ref. 5). The frequency of observations by the Minitrack averages about 6/day, giving a "folding" frequency of 3/day and aliasing frequencies for 1 cycle/day of 5, 7, 11, 13, 17, 19, etc. cycles/day (Ref. 9). None of these frequencies are close enough to the 10.7 cycles/day, etc. to be a likely cause of difficulty for the long record of data available, however, the non-uniform distribution of observations may enhance the distortion of estimates of coefficients of lower frequency variations.

Luni-solar attraction, radiation pressure, drag, and Earth tides do not appear to give rise to any marked daily or semi-daily periods in the orbit, (unless there is a pronounced longitudinal variation in atmospheric density due to the funneling effect of the geomagnetic field on solar charged particles). The dominant effect of drag is best characterized as a "noise" of continuous spectrum, from which the discrete spectrum caused by the gravitational terms should be resolved by a sufficiently long record.

In class (6) error might possibly arise because the reference orbits are computed for seven-day periods. The orbit determination finds a secular drag coefficient and parameters of a rotating Hansen ellipse such that, in conjunction with specified values of kM, J_{20}, and J_{40} variations of the satellite position are most closely accounted for. The most prominent of these variations are expressed as secular changes in the cyclic variables M, ω, Ω; if the *net* changes in these variables over the one-week period were in part due to a J_{nm}, K_{nm} which we are estimating, then the orbit determination procedure will contaminate estimates made from residuals with respect to the orbit. This contamination would be a maximum for J_{nm}, K_{nm} causing variations of frequency $(2I + 1)/2W$, where I is an integer and W is the duration covered by the orbital determination, and would be zero for J_{nm} causing variations of frequency I/W. (Ref. 10). For precisely seven-day periods without overlap contamination peaks should exist for 2.071, 1.927, 1.071, 0.927 cycles/day: all of which are fairly distant from the frequencies of primary interest: 2.028 and 1.014 cycles/day.

Errors in classes (2), (4) and (5) the electronic environmental effects position and orientation error and instrumental effects, are most easily visualized as variations in the observed direction cosines l, m. We should expect that the most prominent peak in those error spectra will be close to 1.000 cycles/day, because of variations in the ionospheric and tropospheric refraction, the geometrical limitations on time of observation, class (3), and the temperature and humidity effects on the antennas and transmission lines of the Minitrack stations. Since most of these variations are all rather irregular, we should expect this peak to be rather broad. The frequency in which we are most interested is 1.014 cycles/day in terms of the orbital elements; to determine whether it might be contaminated by the refraction effects, however, we must first apply the various rotation matrices in Eq. (10) to $d\mathbf{E} = \mathbf{C}_{EG}\{J_{nm}, K_{nm}\}$.

Since Eq. (10) is rather complicated, we shall make this transformation only to the first approximation—i.e., drop all terms with coefficients including the eccentricity or powers thereof, and make a further abbreviation in the form of a notation:

$$
\begin{aligned}
(q_1 q_2 q_3 \cdots) &= \prod_{i=1}^{n} k_i \begin{Bmatrix} \cos \\ \sin \end{Bmatrix} \{\dot{q}_i t + \epsilon_i\} \\
&= \frac{K}{2^n} \sum_{j=1}^{2^n} \left\{ \begin{vmatrix} \cos \\ \sin \end{vmatrix} \right\} \{\dot{r}_j t + \epsilon_j\},
\end{aligned} \tag{11}
$$

where $K = \prod_{i=1}^{n} k_i$ and $\dot{r}_j = \prod_{i=1}^{n} (\pm\dot{q}, \pm\dot{q}_2 \pm \cdots \pm\dot{q}_n)$. Then

$$
d\mathbf{E}^T = \{(m\Omega - m\theta), (m\Omega - m\theta), (m\Omega - m\theta), 0, (m\Omega - m\theta), (m\Omega - m\theta)\}
$$

and

$$
\mathbf{Q}^T = \{(M), (M), 0\}, \text{ etc.}
$$

In the various rotations applied in Eq. (10), $R_1(-i)$, $R_3(\lambda)$, $R_3(\pi/2 - \phi)$ and $R_3(\pi/2)$ have constant arguments, and therefore constitute phase shifts which do not introduce any new frequencies. As it turns out, these phase shifts are important to making a solution possible, but for the present we shall ignore them—so that transforming from dE to $d\begin{Bmatrix} l \\ m \end{Bmatrix}$ is the same as to $\frac{1}{\rho} dU_G$, so far as frequencies are concerned. Carrying out the various multiplications, we get, substituting $S = m\Omega - m\theta$:

$$
\begin{aligned}
d\begin{Bmatrix} l \\ m \end{Bmatrix}_{\text{COMP}} &= \frac{1}{\rho} dL = \{(0) + (\theta\omega\Omega M) + (\omega M) \\
&\quad + (\theta\theta\omega\omega\Omega\Omega MM) + (\omega\omega MM) + \cdots\} \begin{Bmatrix} dl_1 \\ dl_2 \end{Bmatrix},
\end{aligned} \tag{12}
$$

where

$$dl_1 = dl_2 = (\theta SM\Omega) + (\theta SM\omega) + (\theta SM\omega\Omega) + (\theta S\omega\Omega MM) + (\theta S\omega\Omega) + (SM) + (S\omega M) + (S\omega) + (S\omega MM) + O(e).$$

Before carrying out the tedious multiplications, we can simplify by applying the various conditions of observation, which we have called class (3):

(1) For a given Minitrack station, the satellite is only observed crossing the meridian plane; i.e. for the right ascension, α, of the satellite,

$$\alpha = \lambda + \theta \tag{13}$$

and

$$\cot(\omega + f) = \cot(\lambda + \theta - \Omega) \cos i. \tag{14}$$

For Vanguard I, neglecting terms of $O(e) = 0.19$ for Vanguard I means setting $M = f$ and $\cos i = \cos 34° \approx 1$, whence

$$M = \lambda + \theta - \Omega - \omega + O(e) \tag{15}$$

(2) At a given Minitrack station, the satellite is observed only when it is within about 22° of the zenith; so that

$$\text{at perigee,} \quad |\phi\ (\text{Satellite}) - \phi\ (\text{Station})| < 2.1° \tag{16}$$

$$\text{and at apogee,} \quad |\phi\ (\text{Satellite}) - \phi\ (\text{Station})| < 8.8°$$

$$\phi\ (\text{Satellite}) = \phi\ (\text{Station}) + O(e)$$

and

$$f = \sin^{-1}\left(\frac{\sin\phi}{\sin i}\right) - \omega + O(e) \tag{17}$$

so

$$\dot{M} = -\dot{\omega} + O(e). \tag{18}$$

Combining Eqs. (18) and (15) gives:

$$\dot{\theta} = \Omega + O(e) \tag{19}$$

and

$$\dot{S} = 0 + 0(e). \tag{20}$$

Equation (20) indicates that at a single station all gravitational perturbations due to terms containing argument $m\lambda$ look alike, to the first order; if they are to be distinguished, it must be by terms of $O(e)$ and higher. It indicates further that the solution for several of the J_{nm}, K_{nm} will depend on the differences in phase shift introduced for different stations by the rotations $R_3\left(\frac{\pi}{2} - \phi\right)$, $R_3(\lambda)$, and that the solution for the gravitational coefficients should be made simultaneously from several stations by least squares, rather than by harmonic analysis. Substituting Eqs. (18), (19), and (20) in (12), we get:

$$\left.\begin{aligned} \frac{1}{\rho} &= (0) + (\Omega\Omega\omega\omega) + (\omega\omega) + (\Omega\Omega\Omega\Omega\omega\omega\omega\omega) \\ &\qquad + (\omega\omega\omega\omega) + O(e) \\ &= \sum_{i,j=0}^{2} 2(i\Omega + j\omega) + O(e) \\ dL &= (\Omega\Omega\omega) + (\Omega\omega\omega) + (\Omega\Omega\omega\omega) + (\Omega\Omega\omega\omega\omega) \\ &\qquad + (\Omega\Omega\omega) + (\omega) + (\omega\omega) + \\ &\qquad + (\omega\omega\omega) + O(e) = \sum_{g=0}^{2}\sum_{h=0}^{3} (g\Omega + h\omega) + O(e). \end{aligned}\right\} \tag{21}$$

The ρ periods in Eq. (21) will appear for all effects which affect the direction cosines through the satellite range, which would include the datum error, dU_0, and, to some extent, the ionospheric refraction error. The dL periods will be peculiar to even-degree longitudinal harmonics in the gravitational field; it is the periods that make these harmonics separable from other effects—in particular, from the electronic environmental and instrumental effects, for which we can expect daily, monthly (change of refraction formula), possibly semi-annual (recalibration), and annual periods.

In view of the foregoing considerations, a least squares solution was attempted using observation equations of the type of 10 simultaneously for the ten even-degree harmonics likely to have greatest effect: J_{22}, K_{22}, J_{41}, K_{41}, J_{42}, K_{42}, J_{61}, K_{61}, J_{62}, K_{62}, which probably include all even-degree terms having effects of ±20 meters or more amplitude in daily and shorter periods. (J_{31}, U_{31} might have a greater effect, as previously mentioned, but is is separable due to the extra ω term in its argument.) However, the result indicated weak conditioning: in general, the combined effect of a set of similar coefficients (e.g., J_{22}, J_{42}, J_{62}) was appreciably smaller than their separate effects, and the coefficients were unreasonably large compared to the statistical estimates from terrestrial gravimetry (Ref. 8). So solutions were made for J_{22}, K_{22}, J_{41}, K_{41} only, and results were obtained of reasonable magnitude:

From obs. 1–1128:

$$J_{22} = +0.27\ (\pm 0.59) \times 10^{-6},$$

$$K_{22} = +2.59\ (\pm 0.61) \times 10^{-6}$$

$$J_{41} = -1.67\ (\pm 0.20) \times 10^{-6},$$

and

$$K_{41} = -0.09\ (\pm 0.23) \times 10^{-6}.$$

From Obs. 1129–2241:

$$J_{22} = -1.43\ (\pm 0.51) \times 10^{-6},$$

$$K_{22} = +0.85\ (\pm 0.58) \times 10^{-6}$$

$$J_{41} = -1.40\ (\pm 0.22) \times 10^{-6},$$

and

$$K_{41} = +.53\ (\pm 0.23) \times 10^{-6}.$$

From Obs. 2242–3077:

$$J_{22} = -0.99\ (\pm 0.75) \times 10^{-6},$$

$$K_{22} = -0.31\ (+0.67) \times 10^{-6},$$

$$J_{41} = +0.36\ (\pm 0.26) \times 10^{-6},$$

and

$$K_{41} = +0.52\ (\pm 0.26) \times 10^{-6}.$$

The uncertainties stated are those obtained in the conventional manner from the least squares solutions. The changes in results from one solution to another are disappointingly large. These observations covered 525 days. The Minitrack stations are recalibrated about once each six months; changes in antenna orientation on recalibration have been as great as 4×10^{-4}, so the foregoing changes in results could be due to variations in the effective orientations of the Minitrack antennas. The uncertainties for a combined solution are therefore better taken as based on the discrepancies between separate sets:

$$J_{22} = -0.69\ (\pm 1.2) \times 10^{-6},$$

$$K_{22} = +1.17\ (\pm 1.2) \times 10^{-6},$$

$$J_{41} = -1.02\ (\pm 0.35) \times 10^{-6},$$

and

$$K_{41} = +0.30\ (\pm 0.35) \times 10^{-6}.$$

Provided the antenna orientations remain stable, Minitrack data should be adequate to determine the leading coefficients of the gravitational field. In any case, whatever, the type of observations used, more analysis in the direction started in this paper is needed to extract all the information existing in satellite observations. In particular, more investigation is needed of the interaction between the gravitationally caused variations in satellite orbits and the position of tracking stations, and of the effect thereon of the non-uniform distribution of observations due to the gesonetrical limitations of the observing system and orbit used.

Acknowledgments

W. D. Kahn has assisted in the formulation of the equations and contributed several suggestions, R. W. Bryant has given valuable advice on the details of the treatment of the Minitrack observations and the computation of the GOP orbits, and Lloyd Carpenter programmed the machine computations.

References

1. O'Keefe, J. A., Eckels, A. and Squires, R. K., "The Gravitational Field of the Earth," *Astron. J.*, **64**, 245–253, 1959.
2. Kozai, Y., "The Gravitational Field of the Earth Derived From the Motions of Three Satellites," *Astron. J.*, **66**, 8–10, 1961.
3. Cohen, C. J. and Anderle, R. J., "Verification of the Earth's 'Pear Shape' Gravitational Harmonic," *Science*, **132**, 807–808, 1960.
4. King-Hele, D. G., "The Earth's Gravitational Potential, Deduced From the Orbits of Artificial Satellites," *Geophys. J.*, **4**, 3–16, 1961.
5. Kaula, W. M., "Analysis of Gravitational and Geometric Aspects of Geodetic Utilization of Satellites," *Geophys. J.*, **4**, 5, 104–133, 1961, and *N.A.S.A. Tech. Note D-572*, 38 pp., 1961.
6. Musen, P., "Application of Hansen's Theory to the Motion of an Artificial Satellite in the Gravitational Field of the Earth," *J. Geophys. Res.*, **64**, 2271–2280, 1959.
7. Moulton, F. R., "*An Introduction to Celestial Mechanics*," The MacMillan Company, New York, 1914, p. 399.
8. Kaula, W. M., "Statistical and Harmonic Analysis of Gravity," *J. Geophys. Res.*, **64**, 2401–2422, 1959.
9. Blackman, R. B., and Tukey, J. W., "*The Measurement of Power Spectra*," Dover Publ. Inc., New York, 1959, pp. 31–33, 68.

Bending Vibrations of a Disk Subjected To Gyroscopic Forces[1]

Leonard Meirovitch[2]

Abstract

The rigid body assumption in the solution of motion of bodies in space, though good as a first approximation, has certain limitations. To explain certain phenomena, such as energy dissipation, one has to extend the analysis and consider elastic deformations. Using expressions for gyroscopic forces derived from the rigid body assumption, an elastic solution for the vibration of a disk is obtained. Analytical expressions for the deflection, bending moment in the radial direction, and vertical force were derived and plotted as a function of the radial distance.

[1] Manuscript received April 21, 1961. From a dissertation submitted in partial fulfillment of the degree of Ph.D. in Engineering at the University of California, Los Angeles.

[2] Staff Engineer, General Products Division Development Laboratory, International Business Machines, Endicott, New York.

I. Introduction

The motion in space of a moment-free rigid body of revolution, with principal mass moments of inertia

A, A, C, consists of steady precession of the symmetry axis about the angular momentum vector, $\mathbf{h}$, fixed in space. The angle between the symmetry, or spin axis, and the direction of the vector $\mathbf{h}$, is called attitude angle and is a constant. A real body, however, is elastic. A vibrating elastic body undergoes stresses and deformations resulting in internal energy dissipation, which, in turn, causes a change in the attitude angle, θ. The assumption is made here, that the elastic deformations are small relative to the undeformed geometry of the body. Furthermore, it is assumed that the rate of change, $\dot{\theta}$, or nutation velocity, is small relative to the precessional velocity, $\dot{\psi}$, and spin velocity, $\dot{\phi}$. The forces causing the elastic vibrations are the gyroscopic or inertial forces.

The problem to be discussed here treats the case of two circular elastic disks connected by a rigid shaft (Fig. 1).

The solution of a circular plate having the inner circular edge clamped, the outer one free, and subjected to gyroscopic forces is to be found. In order to determine the gyroscopic forces, an expression for the acceleration at any point, P, must be derived.

The acceleration is expressed in terms of the initial angular velocity, ω_0, and the attitude angle, θ, treated as a parameter.

II. The Acceleration Expression

Since only the rotational motion is of interest and there is no relative motion in rigid bodies, the acceleration of any point, P, is given by:

$$\mathbf{a}_P = \boldsymbol{\omega} \times \boldsymbol{\omega} \times \mathbf{R} + \dot{\boldsymbol{\omega}} \times \mathbf{R}. \qquad (1)$$

where $\boldsymbol{\omega}$ and $\dot{\boldsymbol{\omega}}$ are the angular velocity and acceleration of the body respectively, and $\mathbf{R}$ is the radial distance to P.

In terms of components along the body axes, 1, 2, 3, the radius vector $\mathbf{R}$ is given by:

$$\mathbf{R} = (r \cos \alpha)\mathbf{i} + (r \sin \alpha)\mathbf{j} + z\mathbf{k}. \qquad (2)$$

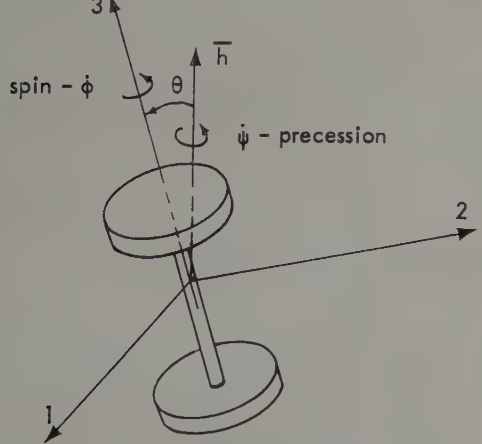

FIG. 1. The body and its angular velocities

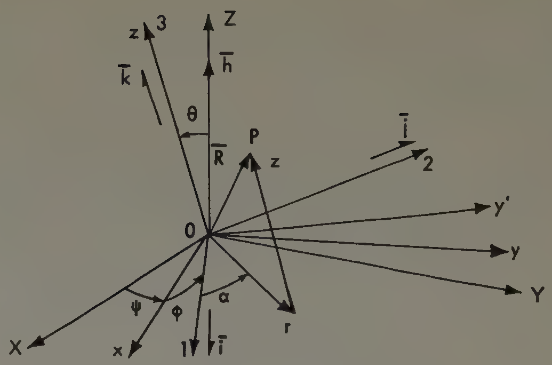

FIG. 2. Coordinates of point P

In Fig. 2, the system XYZ is fixed in space and the angular momentum vector, $\mathbf{h}$, is taken along the Z axis. The xyZ system is obtained by rotation in the XY plane by an angle, ψ. System $xy'z$ results from rotation of system xyZ about the node axis, by an angle θ. System 1, 2, 3 is attached to the body and rotates with respect to system $xy'z$ with angular velocity $\dot{\phi}$ while the direction of axis 3 coincides with the one of z at all times. It follows from Figs. 1 and 2 that the angular velocity components along the body axes, are:

$$\omega_1 = \dot{\psi} \sin \theta \sin \phi,$$

$$\omega_2 = \dot{\psi} \sin \theta \cos \phi, \qquad (3)$$

and

$$\omega_3 = \dot{\phi} + \dot{\psi} \cos \theta.$$

Euler's equations for rotational motion in space can be written in vector form,

$$\mathbf{M} = \frac{d}{dt}(\mathbf{h}), \qquad (4)$$

in which $\mathbf{M}$ is the external moment vector and $\mathbf{h}$ the angular momentum vector given by

$$\mathbf{h} = A(\omega_1\mathbf{i} + \omega_2\mathbf{j}) + C\omega_3\mathbf{k}. \qquad (5)$$

In the above, A and C are the mass moments of inertia about the pitch and spin axes, respectively.

It can be shown from Eqs. (4) that, if there are no external moments applied:

$$\omega_3 = \text{const}, \qquad (6)$$

$$\theta = \text{const}, \qquad (7)$$

$$\dot{\psi} = \frac{C\dot{\phi}}{(A - C) \cos \theta}, \qquad (8)$$

and

$$\dot{\psi} = \frac{C}{A} \frac{\omega_3}{\cos \theta}. \qquad (9)$$

In reality, $\dot{\theta}$ is not zero but very small compared to $\dot{\psi}$ or $\dot{\phi}$. With this in mind, the angular acceleration components become:

$$\dot{\omega}_1 \cong \dot{\psi}\dot{\phi} \sin \theta \cos \phi,$$

$$\dot{\omega}_2 \cong -\dot{\psi}\dot{\phi} \sin \theta \sin \phi, \tag{10}$$

and

$$\dot{\omega}_3 \cong 0.$$

The precession and spin velocities $\dot{\psi}$ and $\dot{\phi}$ can be expressed in terms of the initial angular velocity, ω_0.

It was shown (Reference 1) that if $\frac{A}{C} > 1$ then $\dot{\theta} > 0$. The case where the spin axis initially coincided with the direction of the angular momentum vector, $\mathbf{h}$, is considered here. This implies that, initially, $\theta \sim 0$ and the magnitude of the constant angular momentum vector is $|\mathbf{h}| = C\omega_0$.

From Fig. 3, the following relations can be written:

$$h_3 = |\mathbf{h}| \cos \theta = C\omega_0 \cos \theta = C\omega_3,$$

and

$$h_{12} = |\mathbf{h}| \sin \theta = C\omega_0 \sin \theta = A\sqrt{\omega_1^2 + \omega_2^2}. \tag{11}$$

One concludes that:

$$\omega_3 = \omega_0 \cos \theta \tag{12}$$

and since

$$\sqrt{\omega_1^2 + \omega_2^2} = \dot{\psi} \sin \theta,$$

it follows that:

$$\dot{\psi} = \frac{C}{A} \omega_0. \tag{13}$$

Substituting Eq. (13) into (8), one obtains

$$\dot{\phi} = \left(1 - \frac{C}{A}\right)\omega_0 \cos \theta. \tag{14}$$

Expressions (13) and (14) introduced into (3) and (10) yield the angular velocity and acceleration components in terms of ω_0. Finally, this leads to the acceleration vector, $\mathbf{a}_P$, if Eq. (1) is used.

$$\begin{aligned}\mathbf{a}_P = \omega_0^2 \Bigg\{ &\left[-r\left(\frac{C}{A}\right)^2 \sin^2\theta \cos\phi \cos(\alpha + \phi) - r\cos^2\theta \cos\alpha + z\left(\frac{C}{A}\right)^2 \sin\theta\cos\theta\sin\phi \right]\mathbf{i} \\ &+ \left[r\left(\frac{C}{A}\right)^2 \sin^2\theta \sin\phi \cos(\alpha+\phi) - r\cos^2\theta \sin\alpha + z\left(\frac{C}{A}\right)^2 \sin\theta\cos\theta\cos\phi \right]\mathbf{j} \\ &+ \left[r\frac{C}{A}\left(2 - \frac{C}{A}\right)\sin\theta\cos\theta\sin(\alpha+\phi) - z\left(\frac{C}{A}\right)^2 \sin^2\theta \right]\mathbf{k} \Bigg\}.\end{aligned} \tag{15}$$

III. Elastic Solution of the Plate

The exciting forces on the system are the inertia or D'Alembert forces. The deformed shape is assumed very close to the undeformed one, so that the real accelerations are approximated by the rigid body

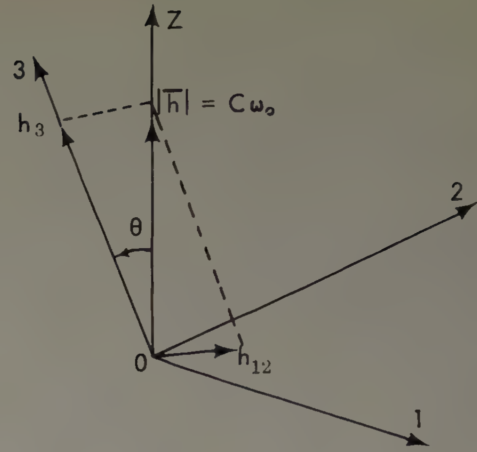

FIG. 3. Angular momentum vector components

accelerations (given by Eq. (15)). Since only the component causing bending is of interest, only the component in the direction of the unit vector $\mathbf{k}$ is retained. From this, only the portion causing vibratory motion is of further interest. Note that the oscillatory terms are the ones containing the angle $\phi = \dot{\phi}t$, where $\dot{\phi}$ is the spin velocity and t denotes the time. Hence

$$\mathbf{a}_P \cong \omega_0^2 r \frac{C}{A}\left(2 - \frac{C}{A}\right) \sin\theta\cos\theta\sin(\alpha + \dot{\phi}t)\mathbf{k}. \tag{16}$$

Denoting by q the distributed force per unit volume and by ρ the mass density one writes:

$$\begin{aligned} q = \rho a_P &= \rho\omega_0^2 r \frac{C}{A}\left(2 - \frac{C}{A}\right)\sin\theta\cos\theta\sin(\alpha + \dot{\phi}t) \\ &= fr\sin(\alpha + \dot{\phi}t) \end{aligned} \tag{17}$$

where:

$$f = \rho\omega_0^2 \frac{C}{A}\left(2 - \frac{C}{A}\right)\sin\theta\cos\theta. \tag{18}$$

As far as the solution of the plate is concerned, f represents a constant.

The distribution of the gyroscopic forces is shown in Fig. 4.

Taking into account the direction of the exciting forces, the plate equation is written:

$$\nabla^4 w + \frac{f}{D_E} r \sin(\alpha + \dot{\phi}t) + \frac{\rho}{D_E}\frac{\partial^2 w}{\partial t^2} = 0, \tag{19}$$

in which D_E is a modified flexural rigidity given by

$$D_E = \frac{D}{h} = \frac{Eh^2}{12(1 - \nu^2)}. \tag{20}$$

Polar coordinates should be used, due to the shape of the boundaries. The variables in Eq. (19) can be separated by the following transformation:

$$w = W(r) \sin(\alpha + \dot{\phi}t), \tag{21}$$

where $W(r)$ is a function of r alone. It will prove convenient to introduce a new parameter, γ, given by:

$$\frac{\rho}{D_E}\dot{\phi}^2 = \gamma^4. \tag{22}$$

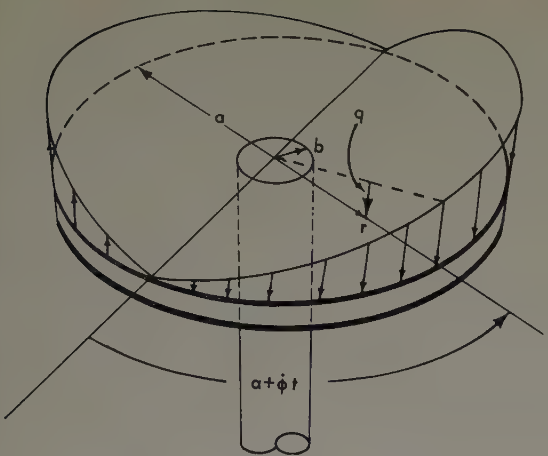

FIG. 4. Gyroscopic force distribution

Introducing Eqs. (21) and (22) into (19), one obtains an equation for $W(r)$ alone, which when it is solved, gives:

$$W(r) = X(1,1)J_1(\gamma r) + X(2,1)Y_1(\gamma r) + X(3,1)I_1(\gamma r) + X(4,1)K_1(\gamma r) + \frac{f}{\gamma^4 D_E} r. \quad (23)$$

In the above, $J_1(\gamma r)$ and $Y_1(\gamma r)$ are Bessel functions of the first order and first and second kind, respectively. $I_1(\gamma r)$ and $K_1(\gamma r)$ are modified, or hyperbolic Bessel functions of the first order and first and second kind respectively. The coefficients, $X(j, 1)$, have to be determined from the boundary conditions. Combining expressions (21) and (23), the solution of Eq. (19) is written:

$$w = \left[X(1,1)J_1(\gamma r) + X(2,1)Y_1(\gamma r) + X(3,1)I_1(\gamma r) + X(4,1)K_1(\gamma r) + \frac{f}{\gamma^4 D_E} r \right] \sin(\alpha + \dot{\phi} t). \quad (24)$$

Solution (24) is subject to boundary conditions. Fig. 4 indicates that at the inner boundary, $r = b$, where the plate is clamped, the deflection and the slope to the deflection curve in the radial direction are zero.

$$w \big|_{r=b} = 0 \quad (25)$$

$$\frac{\partial w}{\partial r}\bigg|_{r=b} = 0 \quad (26)$$

At the outer boundary, $r = a$, the plate is free, so that the bending moment in the radial direction and the vertical force on areas normal to r are zero

$$M_r = D\left[\frac{\partial^2 w}{\partial r^2} + \nu\left(\frac{1}{r}\frac{\partial w}{\partial r} + \frac{1}{r^2}\frac{\partial^2 w}{\partial \alpha^2}\right)\right]\bigg|_{r=a} = 0 \quad (27)$$

and

$$V_r = -D\left[\frac{\partial}{\partial r}\nabla^2 w + \frac{(1-\nu)}{r}\frac{\partial}{\partial \alpha} \cdot \left(\frac{1}{r}\frac{\partial^2 w}{\partial r \partial \alpha} - \frac{1}{r^2}\frac{\partial w}{\partial \alpha}\right)\right]\bigg|_{r=a} = 0. \quad (28)$$

The four boundary conditions, Eqs. (25), (26), (27) and (28), yield four simultaneous equations for the coefficients $X(j, 1)$. The four equations are of the type:

$$A(i,j)X(j,1) = B(i,1), \quad (29)$$

where summation over j is implied.

The boundary condition Eq. (25) leads to:

$$\begin{aligned} A(1,1) &= J_1(\gamma b), \\ A(1,2) &= Y_1(\gamma b), \\ A(1,3) &= I_1(\gamma b), \\ A(1,4) &= K_1(\gamma b), \end{aligned} \quad (30)$$

and

$$B(1,1) = -\frac{f}{\gamma^4 D_E} b.$$

From boundary condition Eq. (26), one obtains:

$$\begin{aligned} A(2,1) &= \gamma b J_0(\gamma b) - J_1(\gamma b), \\ A(2,2) &= \gamma b Y_0(\gamma b) - Y_1(\gamma b), \\ A(2,3) &= \gamma b I_0(\gamma b) - I_1(\gamma b), \\ A(2,4) &= -\gamma b K_0(\gamma b) - K_1(\gamma b), \end{aligned} \quad (31)$$

and

$$B(2,1) = -\frac{f}{\gamma^4 D_E} b.$$

After more laborious manipulations, boundary condition Eq. (27) yields:

$$\begin{aligned} A(3,1) &= -\frac{(1-\nu)}{\gamma a} J_0(\gamma a) + \left[\frac{2(1-\nu)}{(\gamma a)^2} - 1\right] J_1(\gamma a), \\ A(3,2) &= -\frac{(1-\nu)}{\gamma a} Y_0(\gamma a) + \left[\frac{2(1-\nu)}{(\gamma a)^2} - 1\right] Y_1(\gamma a), \\ A(3,3) &= -\frac{(1-\nu)}{\gamma a} I_0(\gamma a) + \left[\frac{2(1-\nu)}{(\gamma a)^2} + 1\right] I_1(\gamma a), \\ A(3,4) &= \frac{(1-\nu)}{\gamma a} K_0(\gamma a) + \left[\frac{2(1-\nu)}{(\gamma a)^2} + 1\right] K_1(\gamma a), \end{aligned} \quad (32)$$

and

$$B(3,1) = 0.$$

Finally, after simplifications, boundary condition Eq. (28) results in:

$$A(4,1) = -\left[1 + \frac{(1-\nu)}{(\gamma a)^2}\right] J_0(\gamma a)$$

$$+\frac{1}{\gamma a}\left[1+\frac{2(1-\nu)}{(\gamma a)^2}\right]J_1(\gamma a),$$

$$A(4,2) = -\left[1+\frac{(1-\nu)}{(\gamma a)^2}\right]Y_0(\gamma a)$$

$$+\frac{1}{\gamma a}\left[1+\frac{2(1-\nu)}{(\gamma a)^2}\right]Y_1(\gamma a),$$

$$A(4,3) = \left[1-\frac{(1-\nu)}{(\gamma a)^2}\right]I_0(\gamma a)$$

$$-\frac{1}{\gamma a}\left[1-\frac{2(1-\nu)}{(\gamma a)^2}\right]I_1(\gamma a), \tag{33}$$

$$A(4,4) = -\left[1-\frac{(1-\nu)}{(\gamma a)^2}\right]K_0(\gamma a)$$

$$-\frac{1}{\gamma a}\left[1-\frac{2(1-\nu)}{(\gamma a)^2}\right]K_1(\gamma a),$$

and

$$B(4,1) = 0.$$

The set of Eqs. (29) can be written in matrix form:

$$[A]\{X\} = \{B\}, \tag{34}$$

in which $[A]$ is a square matrix, and $\{X\}$ and $\{B\}$ are column matrices.

The solution of Eq. (34) is readily obtained if one premultiplies both sides by the inverse of matrix $[A]$, i.e.,

$$\{X\} = [A]^{-1}\{B\}. \tag{35}$$

The above expression gives the coefficients, $X(j,1)$, which, when introduced into Eq. (24), yields the complete solution for the deflection, w.

Making use of Eqs. (27) and (28), one can write equations for the bending moment, M_r, and vertical force, V_r:

$$M_r = \gamma^2 D\left[X(1,1)\left\{-\frac{(1-\nu)}{\gamma r}J_0(\gamma r)\right.\right.$$

$$\left.+\left[\frac{2(1-\nu)}{(\gamma r)^2}-1\right]J_1(\gamma r)\right\}$$

$$+X(2,1)\left\{-\frac{(1-\nu)}{\gamma r}Y_0(\gamma r)\right.$$

$$\left.+\left[\frac{2(1-\nu)}{(\gamma r)^2}-1\right]Y_1(\gamma r)\right\}$$

$$+X(3,1)\left\{-\frac{(1-\nu)}{\gamma r}I_0(\gamma r)\right. \tag{36}$$

$$\left.+\left[\frac{2(1-\nu)}{(\gamma r)^2}+1\right]I_1(\gamma r)\right\}$$

$$+X(4,1)\left\{\frac{(1-\nu)}{\gamma r}K_0(\gamma r)\right.$$

$$\left.\left.+\left[\frac{2(1-\nu)}{(\gamma r)^2}+1\right]K_1(\gamma r)\right\}\right]$$

$$\cdot\sin(\alpha+\phi t)$$

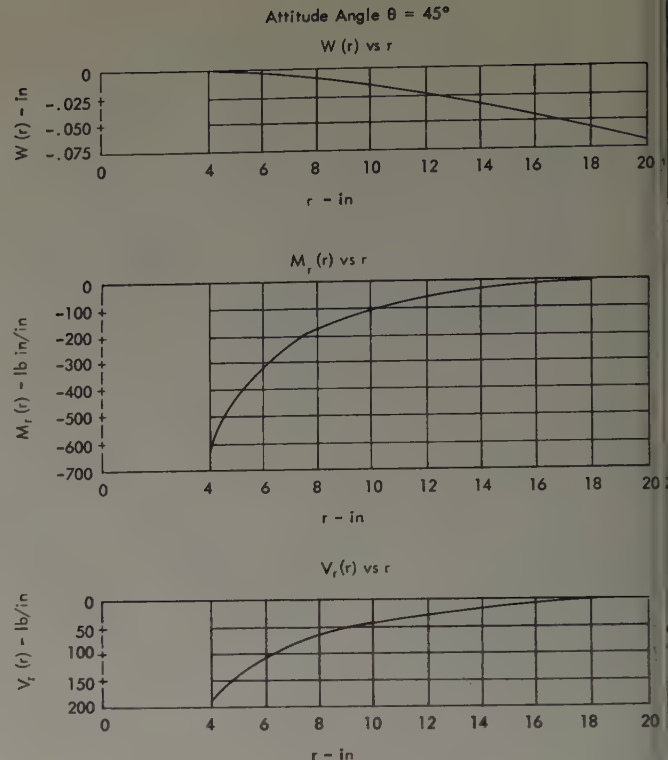

FIG. 5. Amplitudes of deflection $W(r)$, bending moment $M_r(r)$, and vertical force $V_r(r)$ as function of radius r.

and

$$V_r = -\gamma^3 D\left[X(1,1)\left\{-\left[1+\frac{(1-\nu)}{(\gamma r)^2}\right]J_0(\gamma r)\right.\right.$$

$$\left.+\frac{1}{\gamma r}\left[1+\frac{2(1-\nu)}{(\gamma r)^2}\right]J_1(\gamma r)\right\}$$

$$+X(2,1)\left\{-\left[1+\frac{(1-\nu)}{(\gamma r)^2}\right]Y_0(\gamma r)\right.$$

$$\left.+\frac{1}{\gamma r}\left[1+\frac{2(1-\nu)}{(\gamma r)^2}\right]Y_1(\gamma r)\right\}$$

$$+X(3,1)\left\{\left[1-\frac{(1-\nu)}{(\gamma r)^2}\right]I_0(\gamma r)\right. \tag{37}$$

$$\left.-\frac{1}{\gamma r}\left[1-\frac{2(1-\nu)}{(\gamma r)}\right]I_1(\gamma r)\right\}$$

$$+X(4,1)\left\{-\left[1-\frac{(1-\nu)}{(\gamma r)^2}\right]K_0(\gamma r)\right.$$

$$\left.\left.-\frac{1}{\gamma r}\left[1-\frac{2(1-\nu)}{(\gamma r)^2}\right]K_1(\gamma r)\right\}\right]$$

$$\cdot\sin(\alpha+\phi t).$$

IV. Numerical Example

The amplitudes of the functions w, M_r, and V_r were evaluated and plotted for the following values:

Attitude angle	$\theta = 45°$
External radius	$a = 20.0$ in
Internal radius	$b = 4.0$ in
Thickness	$h = 0.5$ in
Mass density	$\rho = 0.00073237$ lb in^{-4} sec^2

Poisson's ratio	$\nu = 0.30$
Young's modulus	$E = 30 \times 10^6$ psi
Initial angular velocity	$\omega_0 = 20$ rad $\sec^{-1}$
Moments of inertia ratio	$C/A = 0.1$

The results are shown in Fig. 5.

V. Conclusions

In many dynamical problems, the rigid body solution can be regarded as a first approximation only. In certain cases, such as with space vehicles, the rigid body analysis is not sufficient and one has to consider the elastic vibrations. In many cases, the acceleration given by Eq. (15) can be used for determining the inertial forces. The assumptions made in the present analysis were the conventional small deflection assumptions and small nutational velocity, $\dot{\theta}$. Both assumptions are justified except when resonance becomes important.

VI. Acknowledgement

The author wishes to thank Prof. W. T. Thomson from University of California, Los Angeles, both for suggesting the problem and for his advice during the course of this investigation.

VII. Symbols

Symbol	*Definition*
A, C	= moment of inertia about pitch and spin axes respectively
$\mathbf{h}$	= angular momentum vector
θ	= attitude angle measured from vector $\mathbf{h}$ to spin axis
$\dot{\theta}$	= nutation velocity
$\dot{\phi}$	= spin velocity
$\dot{\psi}$	= precession velocity
P	= arbitrary point
$\mathbf{a}_p$	= acceleration vector
$\boldsymbol{\omega}$	= angular velocity vector
$\dot{\boldsymbol{\omega}}$	= angular acceleration vector
$\mathbf{R}$	= radius vector
1, 2, 3	= body axes
$\mathbf{i}, \mathbf{j}, \mathbf{k}$	= unit vectors along body axes
r, α, z	= polar coordinates
$X\ Y\ Z$	= fixed axes in space
$x\ y\ Z$	= coordinates system
$x\ y'\ z$	= coordinates system
$\omega_{1,2,3}$	= angular velocity components about body axes
$\mathbf{M}$	= moment vector
$\dot{\omega}_{1,2,3}$	= angular acceleration components about body axes
$h_{12,3}$	= angular momentum components
$\lvert \mathbf{h} \rvert$	= angular momentum magnitude
ω_0	= initial angular velocity
ρ	= mass density
q	= distributed force
w	= plate deflection
$W(r)$	= amplitude of plate deflection
D	= plate flexural rigidity
E	= Young's modulus
h	= plate thickness
ν	= Poisson's ratio
a, b	= outer and inner radius of plate
M_r	= bending moment in radial direction
V_r	= vertical force on plane with normal in the radial direction

VIII. References

1. Thomson, W. T. and Reiter, G. S., "Attitude Drift of Space Vehicles", *The Journal of The Astronautical Sciences* Volume VII, Number 2, Summer, 1960.
2. Morse, P. M., "Vibration and Sound", *McGraw-Hill*, New York, 1948, pp. 172–213.
3. Timoshenko, S., "Theory of Plates and Shells", *McGraw-Hill*, New York, 1940, pp. 257–266.
4. Wang, C. T., "Applied Elasticity", *McGraw-Hill*, New York, 1953, pp. 276–282, 291–294.
5. Synge, J. L. and Griffith, B. A., "Principles of Mechanics," *McGraw-Hill*, New York, 1949, pp. 337–359, 418–447.
6. Gray, A., Mathews, G. B., and MacRobert, J. M., "A Treatise on Bessel Functions and Their Applications to Physics", *MacMillan*, London, 1931, pp. 9–27, 264–317.
7. Carslaw, H. S. and Jaeger, J. C., "Operational Methods in Applied Mathematics", *Oxford University Press*, London, 1953, pp. 348–352.
8. Bowman, F. "Introduction to Bessel Functions", *Dover*, New York, 1958, 135 p.

IN APPRECIATION

The Journal of the Astronautical Sciences is published quarterly through the contributions of various companies within the space industry. These manufacturers through the use of various pages of the Astronautical Science Review, the sister publication of the Journal have brought to the attention of our readers the many and varied products of this industry.

At this time the Society wishes to express its appreciation to these companies for their support this past year and looks forward to a continued pleasant association with them.

The following is a list of those who have contributed to the support of the American Astronautical Society:

Corporate Members

ACF Electronics
Alpha Corporation
AVCO-Everett Research Laboratory
Boeing Airplane Company
Chance Vought Aircraft
Douglas Aircraft Company
Fairchild Aircraft
General Electric Company
Grumman Aircraft Engineering Corp.
Intercontinental Mfg. Company
Kearfott, Div. General Precision
Lockheed Aircraft
Martin Company
McDonnell Aircraft Corp.
Northrop Corporation
Radio Corporation of America
Republic Aviation
Sperry Gyroscope Company
Temco Aircraft
Varo Manufacturing Company

Universities Receiving THE JOURNAL OF THE ASTRONAUTICAL SCIENCES

University of Alabama
University, Alabama

University of Arizona
Tucson, Arizona

Adelphi College
Garden City, New York

Boston University
Boston, Massachusetts

California Inst. of Technology
Pasadena, California

University of California
Berkeley, Los Angeles, Calif.

Carnegie Inst. of Technology
Pittsburgh, Pennsylvania

Case Inst. of Technology
Cleveland, Ohio

Chipola Junior College
Marianna, Florida

Clemson Agricultural College
Clemson, South Carolina

Colorado State University
Fort Collins, Colorado

Cornell University
Ithaca, New York

Fairleigh Dickinson University
Teaneck, New Jersey

Florence State College
Florence, Alabama

Florida State University
Tallahassee, Florida

Georgia Inst. of Technology
Atlanta, Georgia

Illinois Inst. of Technology
Chicago, Illinois

University of Illinois
Chicago, Illinois

R.P.I. Hartford Graduate Ctr.
East Windsor Hill, Connecticut

Iowa State University
Iowa City, Iowa

Purdue University
Lafayette, Indiana

University of South Carolina
Columbia, South Carolina

Southern Methodist University
Dallas, Texas

Stanford Research Institute
Menlo Park, California

Stanford University
Stanford, California

University of Texas
Austin, Texas

Union College
Schenectady, New York

USMA
West Point, New York

USNA
Annapolis. Maryland

Johns Hopkins University
Applied Physics Laboratory
Silver Spring, Maryland

Lafayette College
Easton, Pennsylvania

Lehigh University
Bethlehem, Pennsylvania

Los Angeles City College
Los Angeles, California

Los Angeles Valley College
Van Nuys, California

Lowell Technological Institute
Lowell, Massachusetts

University of Michigan
Ann Arbor, Michigan

University of Minnesota
Minneapolis, Minnesota

New York University
New York, New York

North Carolina State College
Raleigh, North Carolina

Northwestern Technological Institute
Evanston, Illinois

Ohio State University
Columbus, Ohio

Pan American College
Edinberg, Texas

University of Pennsylvania
Philadelphia, Pennsylvania

Polytechnic Inst. of Brooklyn
Brooklyn, New York

Princeton University
Princeton, New Jersey

San Francisco State College
San Francisco, California

San Jose State College
San Jose, California

U. S. Navy Postgraduate School
Monterey, California

University of Utah
Salt Lake City, Utah

University of Washington
Seattle, Washington

University of Wisconsin
Madison, Wisconsin

College of Aeronautics
Cranfield Bletchley Bucks, England

Istituto Universitario Navale
Napoli, Italy

University of Tokyo
Chiba-Ken, Japan

MUrray Hill 2-3383

AMERICAN ASTRONAUTICAL SOCIETY

516 FIFTH AVENUE, NEW YORK 36, NEW YORK

OFFICE RECORD

REC'D.	
REC'D.	
ACK.	
R.R.	
ELECT.	
GRADE	
DATE	
NO.	

APPLICATION FOR MEMBERSHIP

TO THE MEMBERSHIP COMMITTEE OF THE AMERICAN ASTRONAUTICAL SOCIETY:

I hereby apply for membership in the American Astronautical Society, and do agree to conform to the Constitution and By-Laws of the Society. The information given on this application is true and correct to the best of my knowledge.

DATE ____________ SIGNATURE IN FULL ____________________________

(Sign with pen—Do not use initials)

BIOGRAPHICAL RECORD

(Please fill in all information by hand lettering or typewriter)

Name ____________________________ Age ________

(First) (Middle) (Last)

☐ Home Address ____________________________

☐ Business Address ____________________________

(Check mailing address)

Home Tel. No. ______________ Bus. Tel. No. ______________

Date of Birth ______________ Place ______________

Sex ______________ Country of Citizenship ______________

Company or Organization with which you are connected ______________

____

Your Title or Position ____________________________

Nature of your Duties, or your Profession or Occupation ______________

____

Name of Technical or Scientific Organizations to which you belong. (State Grade of Membership) ________

____

____

If you are a Licensed or Registered Engineer or other Professional Specialist, give Title of such License and State in which Registered ____________________________

____

EDUCATIONAL RECORD

College or University	Dates of Attendance	Major Subject	Degree Rec'd & Da

Other

Awards, Fellowships, Scholarships or other Honors Received (Give Dates and Citations)

State Titles of Scientific Papers and When and Where They Were Presented and/or Published

REFERENCES

List at least four references familiar with your activities. Complete addresses of non-members must be su plied. However, references need not be A.A.S. members.

1.
2.
3.
4.
5.

Grade of Membership for Which You Apply

PROFESSIONAL RECORD

(Needs only to be completed by Applicants for the Following Grades: Affiliate Member, Member, or Ass ciate Fellow.)

Give a brief outline of your Industrial, Academic or Related Experience. Use additional sheets necessary.

Date, From - To (year only)	Name of Affiliation and Description of Duties

Format of Technical Papers for THE JOURNAL OF THE ASTRONAUTICAL SCIENCES

The Editors will appreciate the cooperation of authors in using the following directions for the preparation of manuscripts. These directions have been compiled with a view toward eliminating unnecessary correspondence, avoiding the return of papers for changes, and reducing the charges made for "author's corrections."

Manuscripts

Papers should be submitted in original typewriting (if possible) on one side only of white paper sheets, and should be double or triple spaced with wide margins. However, good quality reproduced copies (e.g. multilith) are acceptable. An additional copy of the paper will facilitate review.

Company Reports

The paper should not be merely a company report. If such a report is to be used as the basis for the paper, appropriate changes should be made in the title page. Lists of figures, tables of contents, and distribution lists should all be deleted.

Titles

The title should be brief, but express adequately the subject of the paper. A footnote reference to the title should indicate any meeting at which the paper has been presented. The name and initials of the author should be written as he prefers; all titles and degrees or honors will be omitted. The name of the organization with which the author is associated should be given in a separate line to follow his name.

Abstracts

An abstract should be provided, preceding the introduction, covering contents of the paper. It should not exceed 200 words.

Headings

The paper can be divided into principal sections as appropriate. Headings or paragraphs are not numbered.

Illustrations

Drawings should be made with black India ink on white paper or tracing cloth, and should be at least double the desired size of the cut. Each figure number should be marked with soft pencil in the margin or on the back of the drawing. The width of the lines of such drawings and the size of the lettering must allow for the necessary reduction. Reproducible glossy photographs are acceptable. However, drawings which are unsuitable for reproduction will be returned to the author for redrawing. Legends accompanying the drawings should be typewritten on a separate sheet, properly identified.

Security Clearance

Authors are responsible for the security clearance by an appropriate agency of the material contained in the papers.

Mathematical Work

As far as possible, formulas should be typewritten. Greek letters and other symbols not available on the typewriter should be carefully inserted in ink. Each such symbol should be identified unambiguously the first time it appears. The distinction between capital and lower-case letters should be clearly shown. Avoid confusion between zero (0) and the letter *O*; between the numeral (1), the letter l, and the prime (′); between alpha and *a*, kappa and *k*, mu and *u*, nu and *v*, eta and *n*.

The level of subscripts and exponents, should be clearly indicated. Vectors will be set in bold face type. Authors should indicate this in their manuscripts by a wavy underscore.

Greek Alphabet

Α α	alpha	(a)		Ν ν	nu	(n)
Β β	beta	(b)		Ξ ξ	xi	(x)
Γ γ	gamma	(g)		Ο o	omicron	(ŏ)
Δ δ	delta	(d)		Π π	pi	(p)
Ε ϵ	epsilon	(ĕ)		Ρ ρ	rho	(r)
Ζ ζ	zeta	(z)		Σ σs	sigma	(s)
Η η	eta	(ē)		Τ τ	tau	(t)
Θ θ	theta	(th)		Υ υ	upsilon	(u)
Ι ι	iota	(i)		Φ $\phi\varphi$	phi	(ph)
Κ κ	kappa	(k)		Χ χ	chi	(ch)
Λ λ	lambda	(l)		Ψ ψ	psi	(ps)
Μ μ	mu	(m)		Ω ω	omega	(ō)

The Orbital Elements

a = semimajor axis
e = eccentricity
☊ = longitude of the ascending node
i = inclination
ω = argument of perifocus
T = time of perifocal passage

Complicated exponents and subscripts should be avoided when possible to represent by a special symbol.

Fractions in the body of the text and fractions occurring in the numerators or denominators of fractions should be written with the solidus as follows:

$$\frac{\cos(\pi x/2b)}{\cos(\pi\alpha/2b)}. \tag{1}$$

The intended grouping of handwritten formulas can be made clear by slight variations in spacing, but this procedure is not acceptable in printed formulas. To avoid misunderstanding, the order of symbols should therefore be carefully considered. Thus:

$(a + bx)\cos t$ is preferable to $\cos t\,(a + bx)$.

In handwritten formulas the size of the braces, brackets, and parentheses can vary more widely than in print. Particular attention should be paid to the proper use of braces, brackets, and parentheses (which should be used in this order). Thus:

$$\{[a + (b + cx)^n]\cos ky\}^2 \tag{2}$$

is required rather than $((a + (b + cx)^n)\cos ky)^2$.

Equations are centered, numbered, punctuated as complete sentences; and referred to in text as (2).

Bibliography

References should be grouped together in a bibliography at the end of the manuscript. References to the bibliography should be made by numerals between square brackets [4].

The following examples show the approved arrangements:

for books—[1] BAKER, R. M. L., Jr. and MAKEMSON, M. W., *An Introduction to Astrodynamics*, Academic Press, New York, 1st ed., 1960.

for periodicals—[2] LAMORE, LEWIS, "Celestial Observations for Space Navigation," J. Astronaut. Sci., 6 (1959), 1–10.